AD-A132 274 VIBRATION RESISTANT QUARTZ CRYSTAL RESONATORS(U) 1/2
FREQUENCY ELECTRONICS INC MITCHEL FIELD NY
B GOLDFRANK ET AL. NOV 82 DELET-TR-79-0272-F
UNCLASSIFIED DAAK20-79-C-0272 F/G 9/1 NL

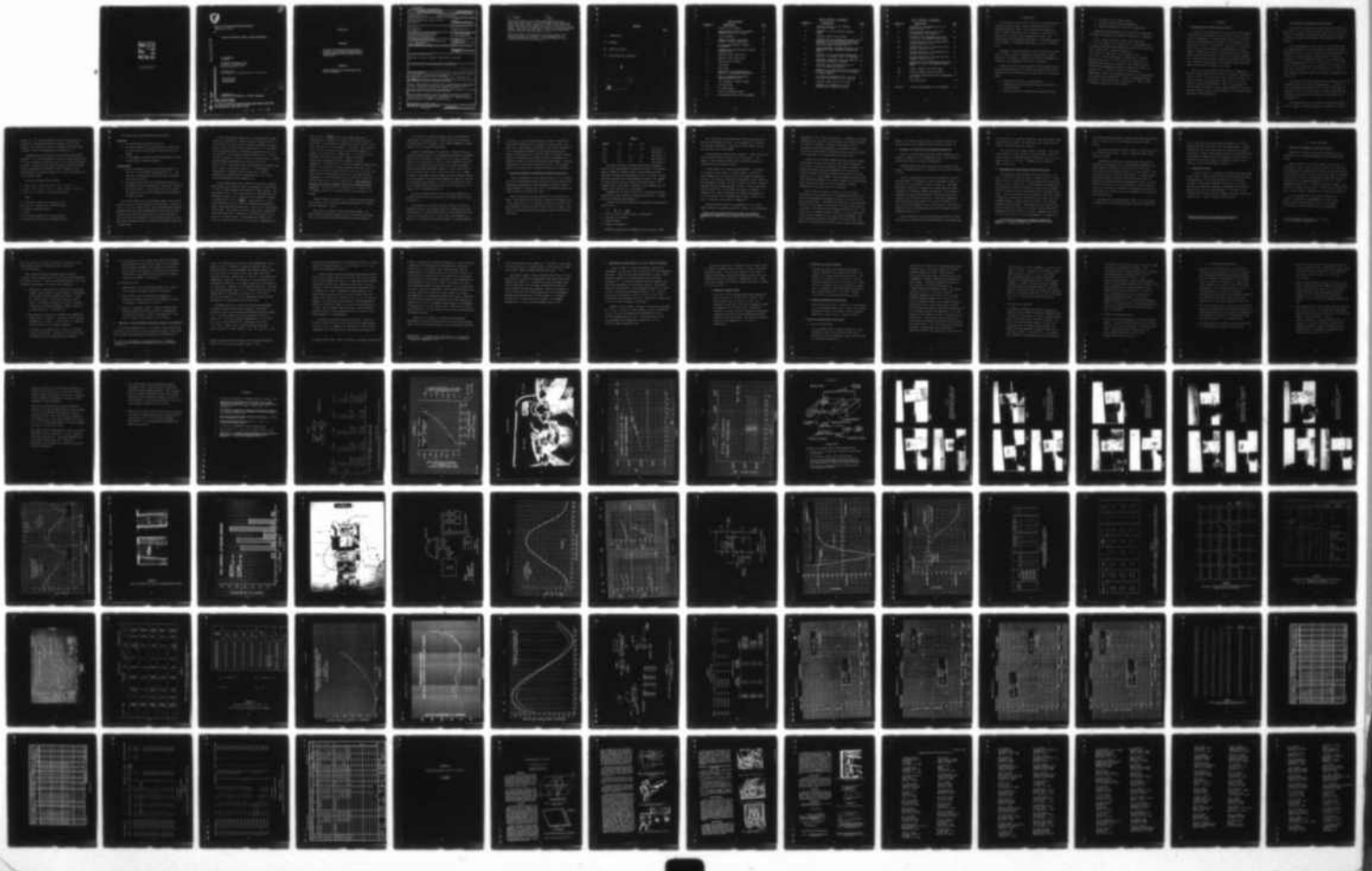

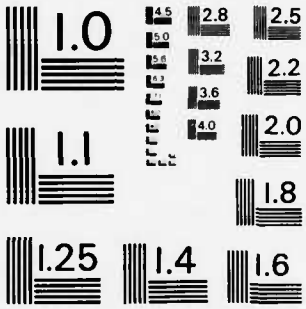

Research and Development Technical Report
DELET-TR-79-0272-F

VIBRATION RESISTANT QUARTZ CRYSTAL RESONATORS

B. Goldfrank
A. Warner

FREQUENCY ELECTRONICS, INC.
55 Charles Lindbergh Blvd.
Mitchel Field, NY 11553

November 1982
Final Report for period 28 Oct 79 - 28 Feb 82

Prepared for:
ELECTRONICS TECHNOLOGY & DEVICES LABORATORY

ERADCOM
US ARMY ELECTRONICS RESEARCH AND DEVELOPMENT COMMAND
FORT MONMOUTH, NEW JERSEY 07703

NOTICES

Disclaimers

The citation of trade names and names of manufacturers in this report is not to be construed as official Government indorsement or approval of commercial products or services referenced herein.

Disposition

Destroy this report when it is no longer needed. Do not return it to the originator.

UNCLASSIFIED

SECURITY CLASSIFICATION OF THIS PAGE (When Data Entered)

REPORT DOCUMENTATION PAGE		READ INSTRUCTIONS BEFORE COMPLETING FORM
1 REPORT NUMBER DELET-TR-79-0272-F	2 GOVT ACCESSION NO. AD A132 274	3. RECIPIENT'S CATALOG NUMBER
4 TITLE (and Subtitle) Vibration Resistant Quartz Crystal Resonators		5. TYPE OF REPORT & PERIOD COVERED Final 28/10/79 to 28/2/82 6. PERFORMING ORG. REPORT NUMBER
7. AUTHOR(s) B. Goldfrank A. Warner		8. CONTRACT OR GRANT NUMBER(s) DAAK20-79-C-0272
9. PERFORMING ORGANIZATION NAME AND ADDRESS Frequency Electronics, Inc. 55 Charles Lindbergh Blvd. Mitchel Field, NY 11553		10. PROGRAM ELEMENT, PROJECT, TASK AREA & WORK UNIT NUMBERS 1L162705AH94101102
11. CONTROLLING OFFICE NAME AND ADDRESS U.S. Army Electronics Technology and Devices Laboratory Attn: DELET-MQ Fort Monmouth, NJ 07703		12. REPORT DATE November 1982 13. NUMBER OF PAGES 83
14. MONITORING AGENCY NAME & ADDRESS(if different from Controlling Office)		15. SECURITY CLASS. (of this report) UNCLASSIFIED 15a. DECLASSIFICATION/DOWNGRADING SCHEDULE

16. DISTRIBUTION STATEMENT (of this Report)

Approved for public release; distribution unlimited

17. DISTRIBUTION STATEMENT (of the abstract entered in Block 20, if different from Report)

Superscript 10 Superscript 9

18. SUPPLEMENTARY NOTES

Low "g" Sensitivity Crystal Units and Their Testing By A. Warner, B. Goldfrank, M. Meirs and M. Rosenfeld.
Further Developments on 'SC' Cut Crystals By B. Goldfrank and A. Warner.

19. KEY WORDS (Continue on reverse side if necessary and identify by block number)

Doubly rotated quartz crystals, Low 'g' sensitivity, Fast warm-up crystal resonators, quartz, quartz crystals, quartz resonators, SC cut, acceleration, vibration, pressure sensitivity.

20. ABSTRACT (Continue on reverse side if necessary and identify by block number)

The principal objectives of this investigation were to provide doubly rotated quartz crystal resonators that exhibit low 'g' sensitivity on the order of 1 $pp10^{10}$ per 'g', and fast warm-up on the order of 1 $pp10^{9}$ in three minutes.

(continued on reverse side)

DD FORM 1 JAN 73 1473 EDITION OF 1 NOV 65 IS OBSOLETE
S/N 0102-014-6601

UNCLASSIFIED
SECURITY CLASSIFICATION OF THIS PAGE (When Data Entered)

20. ABSTRACT

Effects of changes in the mounting orientation have been investigated with respect to the magnitude of the acceleration sensitivity vector, for ϕ angles of 21.95°, 23.75° and 25.00°, using 5 MHz/5th overtone plano-convex and bi-convex quartz crystal blanks. The mounting technique was three-point thermo-compression bonding; the mounts were 90° apart. A new thermo-compression bonding ribbon was evaluated and instituted.

5 MHz and 10 MHz, third overtone crystals and 20 MHz fifth overtone crystals were measured for the magnitude of the acceleration sensitivity vector. Improved methods of x-ray orientation were also investigated.

CONTENTS

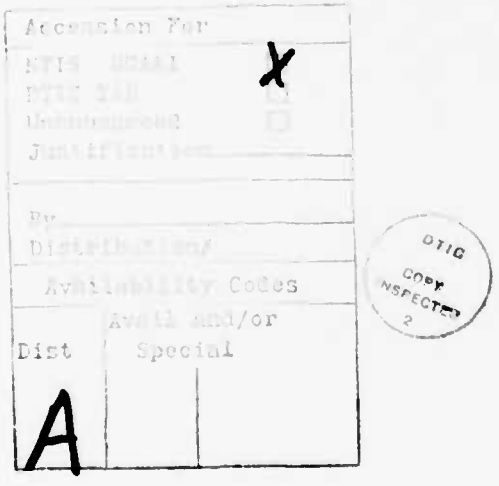

LIST OF FIGURES

LIST OF FIGURES - (CONTINUED)

LIST OF FIGURES - (CONTINUED)

I. INTRODUCTION

The principal object of this contract was the development of vibration resistant quartz crystal resonators of the SC or "stress compensated" type. In this regard an improvement of about 1 order of magnitude, from a few parts in 10^9 per g to a few parts in 10^{10} per g, was accomplished at 5 MHz. The limited number of experiments performed on 10 and 20MHz crystals did not result in a comparable improvement in their "g" sensitivity.

Attempts to correlate particular low "g" sensitivity crystal units to specific design or assembly variations was, in most instances, unsuccessful. Although the yield was increased, the reasons for the improvement are not well understood.

During the course of the investigation many problems of design and measurement had to be solved, and contributions to the state-of-the-art are believed to have been made in the following areas:

1. Accurate mounting of the crystal plate.
2. Measurement of the acceleration sensitivity vector by the "2g" method.
3. Design of circuts to suppress the unwanted "B" mode.

4. Accurate cutting of quartz blanks.

5. Accurate X-ray orientation measurements.

6. Frequency adjustment at controlled temperatures.

Separate measurements were also carried out to investigate the effects of pressure and temperature gradients on frequency.

Of 42, 5 MHz 5th overtone crystal units tested with $\phi = 23.75°$ or higher on this contract (data not presented here), the average magnitude of the acceleration sensitivity vector was $4.03 \times 10^{-10}/g$ with a standard deviation of $1.05 \times 10^{-10}/g$. There were 17 units between 1 and $3 \times 10^{-10}/g$. The test methods were insufficient to resolve anything closer than $1 \times 10^{-10}/g$, and final figures will be determined when units are installed in their respective final oven-oscillator packages and allowed to stabilize. Yields of crystal units $3 \times 10^{-10}/g$ or better of 70% have been experienced in some lots, although the lots were not large enough to be statistically significant. The data is presented only as evidence of a possible solution to the problem. Figure 1 shows the crystal designs used on this contract.

II. PROGRESS

A. Orientation and Cutting of Quartz Blanks

In the cutting of blanks from the quartz bars every attempt has been made to accurately cut blanks so that little or no correcting is necessary. To this end, each bar has its -X surface and one Z surface made flat and parallel to the underlying crystal plane to within 1 minute of arc. Correction at this stage can be more accurately and easily accomplished than at later stages. Mechanical orientation is then carried out by fixtures that can be set to well within 1 minute of the desired orientation. Both sawing and grinding techniques have been used to produce uniformly oriented blanks. The grinding technique is also used to make small corrections if necessary.

The SC cut crystal design has an inflection temperature near 95°C, making angle control critical at turnover temperatures from 80 to 95°C. For this reason, some crystals have been cut to raise the inflection temperature to near 110 C, with little change in overall characteristics. Figure 2 illustrates this fact by showing the range of angle control required to obtain the necessary turnover range. We have assumed a 10°C window as being adequate for most applications.

Use of X-rays to Measure Orientation Angles

Two methods of measuring the quartz plate orientation have been used. The first using an existing X-ray goniometer set for "AT cut" measurements, and the second using an X-ray goniometer dedicated to "SC cut" measurements. Both systems are shown in Figure 3.

For the measurement of SC cut plates on an AT type X-ray, our system consists of tilting the blank to "undo" the Ø angle and permit the use of the 01.1 plane as in the measurement of an AT blank. The crystal blank is then rotated -14° about its thickness so that its measured θ" angle is even closer to that of the reference plane, 38° 12.7', than the AT cut. This -14° angle is the "natural" angle of the blank as cut from an X, Y, Z bar. The exact angle is $\psi = \tan^{-1} (\tan \phi \sin \theta)$. A similar technique is used to measure the Ø angle, independent of the value of θ.

The blanks are cut from a highly corrected quartz bar, using the same θ" angle as in the X-ray measurement. In effect, we have uncoupled the two angles, Ø and θ, and the angle setting on the saw table, θ", is the same as the angle read on the X-ray goniometer, thus permitting an operator to easily make small corrections in θ.

The measured angle Ø' is related to Ø by the know angle of the 01.1 plane. The measured angle θ" is related to θ by the

value of $\emptyset$. The X-ray goniometer which we use measures $\emptyset'$ by reference to a standard and reads in degrees, minutes, and seconds. θ'' is similarly read on a micrometer dial that reads in inches, 0.0001" corresponding to 2 seconds of arc.

A program has been written for the hand-held Sharp EL5100 Calculator. It is only necessary to enter the scale reading from the X-ray goniometer and push one button for the specified angles to appear. Conversion from degrees, minutes, seconds to decimal degrees, comparison with reference crystal readings, inter-relationships of the various angles, etc., are all carried out by the single key stroke.

The actual programs are as follows:

1. $f(AB) = \tan^{-1}$ (tan ((A-B) X D) + 36.3) X Cos C = θ
2. $f(EF) = \sin^{-1}$ (sin (E → deg - F → deg - 18.45) ÷ .7857) = $\emptyset$
3. $\theta'' = 36.3 + (A-B) \times D$, for saw table setting

Where:

A = X-ray dial reading for θ, unknown crystal

B = X-ray dial reading for θ, reference crystal

C = $\emptyset$ angle in decimal degrees

D = .0555

E = X-ray dial reading for $\emptyset$, unknown crystal

F = X-ray dial reading for $\emptyset$, reference crystal

The advantages and disadvantages are as follows:

Advantages:

1. The method used an existing AT set-up.
2. The angle measured, θ", was identical to the angle set on the saw table, making angle correction direct and simple.
3. It was capable of making absolute measurements, as well as ones using a reference standard.

Disadvantages:

1. The tilt necessary to bring the AT X-ray plane (01.1) vertical to the goniometer table was about 15°. This made the data measurement very sensitive to the reference flat (Psi) angle.
2. Calculating Theta from Theta double prime required a knowledge of Phi and calculation of "turn over" required both Theta and Phi. (By the term "turn over" we mean the temperature at which the temperature coefficient of frequency is zero).

The second method, which is preferable, makes use of a very precise, universal, double crystal X-ray goniometer. The sensitivity is ten (10) seconds of arc. Some new approaches have been developed which simplify the measurement of Phi, Theta and Psi, and what may be even more significant a way has been found to relate the turnover temperature of the finished crystal to a single angular measurement with no calculations necessary other than a simple graph.

In the new method of measuring, the crystal blank is considered as a rotated X-cut, making Phi about 8° rather than 22°. This derives, of course, from the three-fold symmetry of quartz. Theta is still near 34° and Psi ranges from 0 to -15° as before. The SC rotational symbol is usually given as YXwl $\phi\Theta\psi$ with ϕ = 21.95° and θ = 33.9° properly called a rotated Y cut. It would be just as correct to refer to the SC as a rotated X-cut, in which case the symbol becomes XYwl $\phi\Theta\psi$ with Phi = 8.05° and Theta = 33.9°. When this is done, the thickness of the plate will be X', and θ' is the rotation about Y'. If the change in nomenclature is confusing, then we could use a rotated Y nomenclature as before and just substitute $(30 - \phi_y)$ in the equations presented for the rotated Y cut.

For the measurement of Phi and Theta we use the 22.3 plane, whose normal lies in the X-Z plane at 34 degrees 17 minutes from X. This is almost exactly Theta and only 8° away from Phi. The Bragg angle is 48°, so the angle between the X-ray beam and the ionization chamber is 48°. The cosine of 34 degrees 17 minutes is .82626, and $\phi = \sin^{-1}\left(\frac{\sin\phi}{.8263}\right)$. Theta prime ($\theta'$) is the angle measured by the X-ray with the crystal blank mounted on a normal vacuum chuck barrel with the Y' (the old X') axis parallel to the table. One Z face of the uncut quartz bar is usually corrected to provide the Y' direction in the blank, which in this case, is not very critical. For measurement of Theta, (θ) a mild tilt, which is not critical, is provided to compensate for ϕ

and $\phi = \tan^{-1}\left(\frac{\tan \theta'}{\cos \phi}\right)$. Phi is the angle measured as described above and Theta (θ') prime is the angle measured by the X-ray. The measurement is made using a non-critical 6° tilt back and with the Z' axis parallel to the Table. The correction for ϕ' and θ' to arrive at ϕ and θ are now small enough to present on a simple sheet of graph paper. A calculator is not necessary once the plots are made. Figure 4 shows the relationship between ϕ and θ for a constant turn over temperature. The upper curve is taken from a paper by Ballato and Iafrate (1976 30th Annual Frequency Control Symposium). As ϕ departs from the AT and goes through FC, ITC, etc. to the SC, the angle θ must be changed accordingly to give the same turn-over temperature. On the same graph, we have plotted the values of θ' which would result in the θ values shown. Note especially that over the range of interest the data is invariant with the value of ϕ. For specified ϕ's from 22° to 24°, θ varies only 0.6 minutes and for ϕ's between 22° and 23° θ varies only .02 minutes.

Figure 5 shows the values of θ', the angle measured directly by the X-ray, for SC turn-over temperatures between 50° and 85°C, for any reasonable ϕ value.

This chart, of course, is for a particular design. For other contours and other frequencies the curve would be the same but the left-hand scale would be shifted up or down slightly.

In a test of 8, 5 MHz 5th overtone units, using Premium Q swept quartz, the values of θ' as read from the X-ray goniometer were 33.540 ±0.012 degrees. The turnover temperature ranged from 60° to 67° as would be predicted.

Should it be desirable to measure the ψ angle, either for measuring existing flats or for determining the place to generate flats, this can be done at either the X' or Z' axes, using the rotated Y cut nomenclature. Using a Y axis reflection, the 02.0 plane, the X' direction of the plate will be some "A" degrees away from the X-ray indication. Where $A = \tan^{-1}(\tan \phi \sin \theta)$. For a ϕ_X of 6.25° (ϕ_Y = 23.75°) and a θ of 33.91°, A = -3.496°. Of course, a prepared crystal standard can also be used to verify this relationship. For reflections from the Z' edge, we can use an X-ray plane whose normal is in the X-Z plane and is 90° from the 22.3 plane used for measuring Phi. Such a plane is the 11.3 plane at 53.75° and Bragg angle 32°.

An X-ray fixture which will both measure and generate an accurate mounting flat on the edge of the crystal plate is shown on Figure 6.

The location of the mounting flats (ψ angle) can also be measured by use of a microscope using both orthoscopic and conoscopic viewing. A Zeiss rotating stage is used which can be read to within 10 minutes of arc. In the normal viewing mode, the quality of the flat and its bearing against a reference edge can

be observed. In the conoscopic mode, an isogyre (sharp black line) can be observed which is related to the direction of the optic axis. The method is as follows: using the Z direction of an SC cut reference standard, find the stage setting for an isogyre crossing bottom to top as the stage is rotated clockwise. Replace the standard with the quartz plate to be measured and rotate the stage to find the same isogyre relationship. A simple calculation will give the location of the flat. The readings taken in this manner have a standard deviation of 0.35 degrees.

C. Mounting Techniques for Reducing Acceleration Sensitivity

There is definitely a relationship between one, the location and size of the mounting points at the edge of the crystal plate, typically accomplished by thermo-compression bonding a ribbon support member to the edge, and, two, the magnitude and direction of the acceleration sensitivity vector.

The configuration used has been that of three points, 90° apart. The bonds should be centrally located on the bonding flat of the crystal and the tool impression should be limited in size and preferably centrally located on the axis of the ribbon. The first five crystals subjected to vibration tests had the following results:

TABLE I

Crystal	R	T	T	
1370	1.4	1.4	1.96	See Figure 7
1371	4.2	-	-	See Figure 8
1373	6.5	1.0	6.6	See Figure 9
1375	7.0	1.8	7.2	See Figure 10
1376	1.4	1.7	2.2	See Figure 11

The need for centrally locating the bonds is apparently caused by the establishment of mechanical couples in the crystal plate. Because the sample is small, re-processed and newly fabricated crystals were photographed prior to sealing. Results were then compared with the photographic evidence. Our present TC bonded crystals use an aluminum clad nickel ribbon. The aluminum side of the ribbon is bonded to the plated edge of the crystal under constant heat and pressure.

Independently, Professor Peter Lee[1] of Princeton University calculated the same location for mounting points (Psi ( ) angle) as we had determined experimentally.

Professor Lee[1] first defined the coefficient of acceleration sensitivity as

$$K_a = \frac{\Delta f}{f_o} \cdot \frac{1}{F} \cdot \frac{d}{f_o/n}$$

F = force on plate = mass of plate x acceleration

f_o = frequency of resonator

n = overtone number

d = diameter of resonator

[1] 34thAnnual Symposium on Frequency Control; Page 403, 1980.

This is similar to the coefficient of force sensitivity K_f. Then for each support position ψ, K_a is computed as a function of acceleration direction. From this, one can obtain $|K_a|$ max, the absolute value of K_a maximum.

This process was repeated for a range of ψ values, and he was able to obtain values of $|K_a|$ max as a function of ψ. See Figure 12, which shows Professor Lee's calculated values as a solid line and FEI's data as points.

A new ribbon for TC bonding been developed[2]. It consists of a stripe of gold coined to a nickel ribbon. A supply of various sample lots of nickel with the gold bonding stripe was received from Technical Materials Incorporated, and was used for our experimental studies. FEI had to anneal the ribbon, since the samples received are approximately 1/4 hard. Initial data shows that the bonds were, at a minimum, equivalent in strength. A diagram of the ribbon is contained in "Further Developments on 'SC' Cut Crystals" by B. Goldfrank and A. Warner, Figures 9, 10 and 11, attached to this report, in Appendix I.

Because the gold stripe ran perpendicular to the ribbon length, methods of precisely cutting the ribbon to the appropriate

[2] Evaluation of Interposed Gold Wire Leads for TC Bonded External HIC Connections; H. N. Keller, Bell Laboratories, Allentown, Pa. and C. E. Apgar, Western Electric Co., Allentown, Pa.

dimensions, ±0.001", had to be worked out. Although we have made completed units, none have had bonds which were exactly centered or uniform in thickness. Extremely close control of all processing and fixturing parameters was needed in order to discover the exact effect of the mounting point size and location on the magnitude of the acceleration sensiivity vector.

Ribbons with the coined triangular stripe along the length, rather than the width have also been used, thus eliminating a very difficult positioning problem at the quartz interface. New welding techniques have been developed at FEI to permit the direct attachment of the gold stripe of the ribbon to the gold-plated pins of a C type header. This eliminates the need for the usual fold and/or removal of the gold to expose the nickel surface. This technique has proved to be very successful, and was implemented on the final test lots of crystals.

Three 5 MHz 5th overtone SC crystal units, which were mounted using nickel ribbons with a lengthwise gold stripe .010" wide were disassembled to observe the nature of the bond to the quartz mounting flat. The bonding was done with a tip temperature of 450°C and a pressure to ten pounds. The size of the tool was .020" wide. The bonded area was slightly larger than .010 x .020 inches, and of a shape as shown on Figure 13. In all cases, particles of quartz adhered to the ribbon after disassembly. Two units similarly mounted were subjected to vibration from 10 to 2000 Hz at vibration levels from 10g to 60g, without any apparent

damage. Pull tests of these bonds are typically higher than those made with Al-Ni ribbons by 36%, as shown in Figure 14.

D. Adjustment to Frequency at the Operating Temperature

The SC cut crystal design has such a poor temperature coefficient of frequency at room temperature that it is necessary to calibrate the unit at an elevated temperature.

Frequency Electronics has fabricated a three position hot tuner. This machine allows us to adjust SC cut crystals to within 0.1 PPM.

The three positions of the tuner are mounted on a fourteen inch base plate and covered by a twelve inch spherical dome. A picture of one of the heads is shown in Figure 15. The heater block and Pi network are removable for easy maintenance and/or changeover to a different header configuration. The filament is shielded (not shown) front and back to eliminate any possible shorting of the internal electronics. The crystal temperature can be continuously monitored and is accurate to within ±1°C. This is more than adequate for any SC cut crystal, since there is normally a 4°C to 6°C range where the crystal frequency does not change more than 1.5 Hz.

The Pi networks all have one common ground as do the inputs and outputs for measuring the crystal frequency. The tuner heads

are connected to an eight pin feed-thru, with three inputs, three outputs and two grounds. All other electrical connections are through a separate twenty pin feed-thru.

The entire tuner is under a laminar flow hood. The vacuum cycle consists of three minutes on a graphite pump, fifteen to twenty minutes on a vac-sorb pump and sufficient time on the ion pump to reach 5×10^{-7} torr. A schematic of the system is shown in Figure 16.

E. Measurement of the Acceleration Sensitivity Vector

Two methods of testing crystal units are currently in use. One is the use of a vibration table to generate known 'g' levels and the other is a static test using the acceleration of gravity, known as a '2g' tipover test. In both methods, the components of the acceleration vector[3] are measured in three mutually perpendicular directions, and the vector magnitude and direction calculated. In initial studies the static method is preferred because it measures the acceleration sensitivity vector apart from any resonance effects. Crystal units are mounted in FEI designed standard oven-oscillators. Improvements have been made by altering the temperature control in the crystal oven and making the temperature setting external to the oven. Temperatures from 40° to 100°C can be set by a 10 turn potentiometer. In addition, a

[3] The Effect of Vibration on Frequency Standards and Clocks, R. L. Filler, USAERADCOM, Proceedings 35th Annual Symposium on Frequency Control, 1981.

3.3 megohm resistor was added in parallel with the crystal terminals, to remove any D.C. bias generated during the warmup period.

2g turnover acceleration tests of normal crystals can be run at the rate of one an hour. Figure 17 shows the type of data that can be taken.

In making 2g turnover tests, particularly where very low acceleration coefficients are to be measured, one observes that false frequency readings of a few parts in 10^{10} often occur due to drift, erratic behavior from initial strain relief, noise, and possibly circuit and cabling variations. In order to separate these variables from the actual acceleration effect on frequency the following method of taking data is used. With the crystal unit mounted in its oven-oscillator and stabilized for one hour, five successive readings of frequencies are taken at 5 second intervals, then the oven is re-oriented by 180°, and five more readings taken.

By repeating this procedure three times, the true acceleration effect for this one orientation can usually be ascertained

even in the presence of drift and noise, however it is still possible to have a 20% error in any given measurement. Further, knowing that the acceleration effect vs. angle in any plane is sinsuoidal in shape, a second check for false or suspected values is provided by using several sets of readings, each 90° apart in the plane of the quartz plate. An example is given for both a good and a difficult measurement in Figure 18.

F. Oscillator Circuits

In the SC design, the orthogonal thickness shear mode, known as the B mode, is more strongly excited than the desired C mode. The suppression of the B mode has been left to the circuit designer.[4] Successfully designed circuits for 5, 10, and 20 MHz have been made which suppress any frequency other than the one for which the circuit was designed. A "B" mode 1/3 the resistance and only 8% removed in frequency will not oscillate in these circuits. Figure 19 shows a typical design.

[4] "Design of Crystal and Other Harmonic Oscillators" by Benjamin Parzen, Wiley Interscience, 1982

III. TESTS AND RESULTS

A. Pressure vs. Frequency of the SC Cut Crystal

Pressure vs. frequency studies were conducted using the hot-tuner with its variable temperature control and excellent vacuum.

Pressure sensitivity tests were made, using a 5 MHz, 5th overtone, SC crystal, with a turnover of 85°C. The crystal unit was inserted into a temperature controlled block inside the high vacuum system, with the flange of the crystal holder in intimate contact with the block. The temperature under high vacuum was controlled at the turnover temperature of 85°C ±0.1°C and independently measured. The greatest temperature change, going from air to vacuum, was less than 1°C, and would account for less than 0.1 Hertz change in frequency at a steady state condition.

It was established that the effect of atmospheric pressure on frequency is approximately +1.5 Hertz, about double reported by Stockbridge[5] for the AT cut crystal. If the curve is nearly linear as shown by Stockbridge,

[5]Vacuum Microbalance Techniques, Vol. 5, 1966, C.D. Stockbridge, Plenum Press.

then 1000 microns of nitrogen, introduced, should have a very small positive effect on frequency, about 0.002 Hertz, (4×10^{-10} Hz/torr).

After flushing the vacuum chamber several times with nitrogen, a base frequency at 85°C in high vacuum was established at 5009280.51 Hertz. A series of experiments was then run. Each experiment was started at the same initial frequency.

a) 500 microns of nitrogen was introduced into the vacuum chamber. The frequency increased almost instantaneously by 0.25 Hertz and then gradually went down 1.5 Hertz. The initial rise is in the right direction, but too large. The frequency decrease with time is believed to be absorption of some contaminant, possibly from the nitrogen feed line. (See Figure 20).

b) 500 microns of nitrogen was introduced and immediately pumped back to 10 microns. The effect was to lower the frequency by 0.1 Hertz. In high vacuum, the frequency slowly returned to the original frequency.

c) 10 microns of nitrogen was very carefully introduced through a bleed valve. There was no significant change in frequency from the established base frequency.

d) A slow steady leak of nitrogen was carefully established at approximately 50 microns per minute, and the frequency versus pressure recorded. The frequency rose initially by 0.05 Hertz at 50 microns, and lowered by 0.50 Hertz at 1000 microns. Upon closing the leak valve the frequency continued to decrease. See Figure 21.

The conclusions are:

1) Contamination in the gas delivery systems is the cause for all negative frequency changes with pressure.

2) Sudden inputs of gas may disturb the temperature equilibrium enough to account for the temporary increase in frequency in experiments "a" and "d".

3) There is no anomalous change in crystal frequency from pressure changes that might occur due to outgassing in the crystal enclosure, as shown in experiment "c". The effect is small, on the order of 4×10^{-10}/torr.

B. Magnitude of the Acceleration Sensitivity Vector vs. Orientation

It has been suggested[6] that if the proper ϕ angle and mounting method were found and used, then a plano-convex crystal blank should have the same good acceleration coefficient as a double-convex

[6]Dr. John Vig, USAERADCOM, private communication - suggestion based on results obtained at USAERADCOM on four-point mounted resonators.

blank. The theoretical ϕ angle for stress compensation is often quoted as 21.95°. Therefore, a group of eighteen 5 MHz, 5th overtone crystal units were prepared from Premium Q swept* quartz with angles near 22° and near 23.75°, both plano-convex and bi-convex, and with ψ angles near -14° and -17°. The results are summarized on Figure 22. The variation in the magnitude of the acceleration coefficient in the radial direction is not enough to be significant. However, in the thickness direction, it is clear that the double-convex shape is 3 to 4 times better, and with the present design is necessary to the goal of 1×10^{-10} per g. The original design at ϕ = 23.75° is marginally better for the magnitude of the acceleration sensitivity vector.

Professor Peter Lee, of the Civil Engineering Department, Princeton University has been most helpful in providing a theoretical basis for the relationship between orientation angles (ϕ, θ, ψ) and the magnitude of the acceleration sensitivity vector, $|\vec{\Gamma}|$. One of his studies[7] indicated that a ϕ of 21.95° and ψ of -25° could provide a $|\vec{\Gamma}|$ considerably less than 1×10^{-10}/g. Crystal units, 5 MHz 5th overtone were made with a ϕ near 21.95° and ψ angles of -23°, -25°, and -27°. The

*Sawyer Research Products, Eastlake, Ohio, Registered Material

[7]Letter, P.C.Y. Lee to A.W. Warner, April 9, 1981

results showed magnitudes of the acceleration sensitivity vector typical of previous designs at ϕ = 23.75° and ψ = -15°. The results are summarized on Figure 23.

A group of quartz blanks was procured from Colorado Crystal Corp.* with a nominal value of ϕ of 21.95° and θ such as to put the turn-over temperature near 50°C. These blanks were prepared from premium Q quartz, not swept, and are 4.6 MHz at the 5th overtone. Twenty of these blanks have been reprocessed at FEI for operation at 5 MHz. The design is double-convex, 2 1/8 diopter per side, and polished. The were divided into five groups of four each, with ψ angles of +5, -5, -10, -15, and -20 degrees. All units were ribbon mounted by thermo-compression bonding at 3 points 90° apart, with two of the points near the Z" axis. The 2g turnover tests were made in four directions radially and one in the thickness direction, in order to give some redundancy to the measurement.

The results are listed on Figures 24 and 25. Figure 24 gives the actual location of the ψ angle to the nearest degree, the value of ϕ to 0.1 degree, the resistance R1, the turn-over temperature, and the magnitude of the acceleration sensitivity

*Colorado Crystal Corp., 2303 W. 8th Street, Loveland, Colorado 80537

vector. In Figure 25, the data is presented in a way to show any correlation of the magnitude of the acceleration sensitivity vector with (1) the spread in the location of the three 90° mounting flats on the quartz plate, (2) the vector direction in the plane of the crystal, and (3) the position of the mounting points relative to the crystal plate flats. The nomenclature is from Gualtieri,[8] A and B are Z" axis, C is normal to Z" axis. The acceleration effect is highly variable, i.e., no correlation was found. The vector magnitudes in the thickness direction were all near $1PP10^{10}/g$ and had only a small effect on the angle and magnitude of the acceleration sensitivity vector. There may be a correlation between the abnormally high vector magnitude of crystal unit D4 and the relatively large errors in the placement of mounting points on that crystal plate, although this is by no means conclusive. In the B series, only one unit was suitable for acceleration testing.

Figure 26 is an attempt to correlate the approximate magnitude of the acceleration sensitivity vector versus mounting angle ψ with one of the theoretical curves of Professor Peter Lee.

[8]DELET-TR-81-5 "A simple method for location of the mounting positions for low acceleration sensitivity SC cut resonators", J. Gualtieri, USAERADCOM, 1981.

If we add the previous data taken at ψ = -25° and ϕ = 21.95, and if we are selective in choosing values, a curve similar in shape can be drawn, showing optimum mounting angle near ψ = 14°.

The group of twenty 5 MHz 5th overtone units with ϕ = 21.95° and various (ψ) angles were reprocessed using gold-stripe nickel ribbons (see Figure 27). Traceability of the individual units was not maintained, but the overall acceleration sensitivity vector magnitude was greatly improved. Omitting two defective units in each case, the original magnitude of the acceleration sensitivity vector was 6.6 x 10^{-10}/g average, 3.11 standard deviation for 15 units and was 4.8 average, 2.35 standard deviation for 17 units of the reprocessed crystal units.

C. Experimental Crystal Units at $\phi = 25°$, 5 MHz 5th Overtone

A group of eight 5.115 MHz 5th overtone units with an experimental ϕ angle of 25° and ψ angles near -15° were processed and tested. Two units are obviously defective, having a large thickness component of the acceleration vector and high resistance, R_1. If these are omitted, then the remaining six units have remarkably low acceleration vectors. The average reading of the magnitude of the acceleration sensitivity vector is $2.64 \times 10^{-10}/g$ with standard deviation of 1.73. Five of the six units are between 1 and $3 \times 10^{-10}/g$, or 83%. This is the best yield experienced so far. Variation in ψ angle from -14° to -18° did not appear to any effect.

Because of this success, the group of crystals was enlarged to 17 units. The data on these crystals is given in Figure 28. For all 17 units, the average vector magnitude is $5.52 \times 10^{-10}/g$ standard deviation 4.46. If the three worst units are eliminated, the average vector magnitude is $3.75 \times 10^{-10}/g$, standard deviation 2.04.

The crystal units with a ϕ angle of 25° were further tested to evaluate the negative effect of using a ϕ angle 3° from that considered optimum. Two units were tested for the effect of temperature gradients, amplitude of vibration (drive level) and infection point of the frequency vs. temperature curve. These results were conpared with those of crystal units having ϕ angles of 21.95° and 23.75°.

(a) Temperature Gradient Effect.

Six crystal units of standard design were selected for test, two each at ϕ = 21.95°, 23.75°, and 25°. They were all given heat runs from 30° to 70°C in an automated slew test box. The rate of temperature change was regulated at 0.75°C per minute. The maximum frequency at turnover for both increasing and decreasing temperature was used to find the temperature gradient effect at this rate of change. The results are shown on Figure 29. The numbers are < 1, 8, and 10^{-9} respectively.

(b) Amplitude of Vibration Effect.

The same six crystal units above were operated at turnover temperature with varying drive levels. The frequency vs. crystal current was plotted for ϕ = 22° and 25°, for currents of 10 μA to 1000 μA, with the frequency normalized at 100 μA (see Figure 30). Below 100 μA, the frequency tends to be unstable, and above 300 μA, the effect of drive level becomes significant with a slope greater than 1 x 10^{-10}/μA. Between 100 and 300 μA, all units behaved about the same.

(c) Frequency-Temperature Characteristic.

Three crystal units with a ϕ angle of 25° were operated over the temperature range of 25 to 180°C. The turnover temperatures are 62, 63, and 65°C, and the inflection temperature is about 122°C, as shown on Figure 31.

D. J Mount and Diamond Mount Crystal Units

1) 10 MHz, third Overtone

"J" and diamond mounts, as shown in Figure 31A, were evaluated on 5 MHz, third overtone, 10 MHz, third overtone and fifth overtones and 20 MHz, fifth overtones for acceleration sensitivity.

One group of 10.054 MHz, third overtone crystals were processed twice. The initial fabrication used the standard diamond notch mount. Electrical and acceleration data were taken. The crystals were then disassembled, cleaned, reprocessed, and acceleration data re-taken. The data is presented in Figure 32. Four additional third overtone crystals, at 10.230400 MHz were processed and tested. The initial plating was done at 7×10^{-8} torr, the final frequency adjustment at 85°C and 5×10^{-7} torr and sealed at pressures between 3×10^{-7} and 5×10^{-7} torr after hydrogen firing. Test results are shown in Figures 33A to 33D. Twenty-eight crystal units at 10.054 MHz were measured for acceleration sensitivity in the same manner as previously described, i.e., by 2g turnover at the rotated X, Y, and Z axes of axes of the crystal plate. The three 90° mounting points are at both ends of the rotated Z axis and the negative end of the rotated X axis. Y is in the direction of the plate thickness. The magnitude of the acceleration sensitivity vector is the square root of the sum of the

squares of the X, Y, and Z components. Figure 34 lists the test results. The average of the absolute value of gamma Γ_{AV} is 10.71 with a σ = 2.97. The crystals were manufactured using the standard techniques developed by Frequency Electronics for epoxy mounted crystals. A diamond notch mount was used. Complete electrical data is contained in Figures 35A and 35B. Data on 30 additional units, one of which was repeated (#4750) is included in Figure 36. As noted, the average was 11.33 x 10^{-10}/g with a standard deviation of 5.89.

2) 5.115 MHz, Third Overtone

Ten chemically polished, plano-convex crystals were supplied to FEI by ERADCOM. These were assembled using "J" mounts, on three posts, 90° apart. The initial data taken, showed large radial acceleration effects. This was due to random mounting caused by the lack of an orientation flat. The data followed, however, the theoretical curve prepared by Professor Peter Lee of Princeton University. (See Figure 12). The crystals were subsequently reprocessed and correctly mounted by

the addition of an orientation flat. The flat was added by X-ray and cross-polaroid techniques. The acceleration results, which we expected to be excellent, were disappointingly bad ranging from 1 to 58 x 10^{10}/g and averaging 35.7 x 10^{10}/g. These crystals were reprocessed a second time and mounted using the cross-polaroid technique and then pasted. The average magnitude of the radial component of the acceleration sensitivity vector was 11.6 x 10^{-10}/g with a standard deviation of 1.83. The average thickness component was 27.6 x 10^{-10}/g with a standard deviation of 7.17. The maximum acceleration effect in the radial direction is given separately from that of the thickness direction because of the high value of the latter.

3) 20 MHz, Fifth Overtone Crystals

Twelve units were constructed using the design shown in Figure 1. The series resistance was less than 100 ohms and the Q was greater than 500,000. Of the five units tested, the average value of $\vec{\Gamma}$ was 6.57 x 10^{-10}/g with a standard deviation of 2.28 x 10^{-10}/g. Complete data is given in Figure 37.

IV. DISCUSSIONS AND CONCLUSIONS

1. The search for an optimum design for acceleration resistant units is continuing. Attempts to associate small manufacturing deviations with poor performance have not succeeded. Some evidence exists to indicate that an increase in the value of the angle beyond 21.95°, perhaps to as high as 25°, can yield a higher percentage of 5 MHz 5th overtone crystal units with coefficients near $1 \times 10^{-10}/g$. Plano-convex crystal designs have shown a high thickness component of the acceleration sensitivity vector which is not balanced out by the mounting variations used so far.

2. 10 and 20 MHz crystal units, which have not yet had TC bond holders designed for them, have not exhibited low acceleration sensitivity vector magnitudes comparable to the TC bonded 5 MHz designs. The 20 MHz design does show some promise as it is a balanced crystal.

3. The "single-angle" X-ray method of measuring SC blanks is proving both easy to carry out and accurate.

4. Gold stripe ribbons with a lengthwise gold stripe can now be successfully welded. Significantly higher yields of 5 MHz 5th overtone crystal units with acceleration sensitivity vectors less than $3 \times 10^{-10}/g$ have been obtained.

5. Tests of thermo-compression bonding using gold stripe nickel ribbons indicate that compared to aluminum clad ribons, pressures can be reduced to 6 pounds from 10 pounds and that tip and stage temperatures can be reduced by 50°C, to 400° and 300°C respectively. Attempts to further reduce the temperature weakened the bond.

6. The indications from a small number of crystal units are that 5 MHz units with $\phi = 25°$ have lower acceleration vector magnitudes and are less sensitive to the mounting angle, ϕ, than those with $\phi = 21.95°$. Since this angle is 3° from the preferred angle, it is necessary to re-evaluate the effect of drive level, temperature gradients, inflection temperature, and impedance level. For example, the impedance level is 20% higher than that of $\phi = 23.75°$.

Further, since some of the best and worst results were obtained from this group it is possible that there is another variable that we have not been able to identify. If this variable is identified in the future, these experiments should be repeated.

Of these four characteristics, that of temperature gradient is the most pronounced, and will have an effect on the time for frequency stabilization following a temperature change. The drive level effect appears to be the same for all units tested, although the 2 units at ϕ = 21.95° showed less tendency for erratic frequency readings at very low drive levels.

The higher inflection temperature of 122°C is a distinct advantage for ease of manufacture of units, especially those operating near 90°C. The higher impedance level will require slightly more care in frequency calibration, but once made, the crystal units should be entirely satisfactory.

7. The 10 MHz crystal units have shown poor results throughout. This is mainly due to the design with secondary effects caused by mounting. This is evident due to the better performance of the 20 MHz crystals which have similar mounting structures, but are of a balanced design. Results were typically $11.3 \times 10^{-10}/g$ with a standard deviation of $5.9 \times 10^{-10}/g$.

8. Testing of six 20 MHz units using the new test set shows an average of the magnitude of the acceleration sensitivity vector of $6.57 \times 10^{-10}/g$ with a standard deviation of 2.28. Improved mounting techniques may improve these results.

REFERENCES

1. 34th Annual Symposium on Frequency Control, Page 403, 1980.

2. Evaluation of Interposed Gold Wire Leads for TC Bonded External HIC Connections; H. N. Keller, Bell Laboratories, Allentown, PA and C. E. Apgar, Western Electric Co., Allentown PA.

3. The Effect of Vibration on Frequency Standards and Clocks, R. L. Filler, USAERADCOM, Proceedings 35th Annual Symposium on Frequency Control, 1981.

4. Design of Crystal and Other Harmonic Oscillators, B. Parzen, Wiley Interscience, 1982.

5. Vacuum Microbalance Techniques, Vol. 5, 1966, C. D. Stockbridge, Plenum Press.

6. Dr. John Vig, USAERADCOM, Private Communication.

7. Letter from P. C. Y. Lee to A. W. Warner, April 9, 1981.

8. DELET-TR-81-5, A Simple Method for Location of the Mounting Positions for Low Acceleration Sensitivity SC Cut Resonators, J. Gualtieri, USAERADCOM, 1981.

FIGURE 1

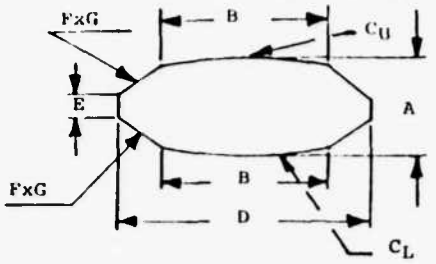

All dimensions in millimeters (inches)

Design No.:	1★	2	3	4	5
Frequency:	5.000 MHz	10.2304 MHz	10.054 MHz	20.000 MHz	10.230 MHz
Overtone:	5	3	3	5	5
ϕ:	23.75	23.75	23.75	23.75	23.75
θ:	33.79	33.97	33.93	34.01	33.97
ψ:	14.80	14.80	14.80	14.80	14.80
Mount:	Ribbon	L.P.D.[1]	L.P.D.[1]	L.P.D.[1]	Diamond Notch
Header:	'C'	TO-8	TO-8	TO-8	'C'
A:	1.864 (.0734)	.526 (.0207)	.536 (.0211)	0.450 (.0177)	.879 (.0346)
B	13.310 (.524)	9.042 (.356)	9.042 (.356)	8.001 (.315)	13.513 (.532)
C_U:	2.125 Diop^2	1.75 Diop^2	1.75 Diop^2	0	1.0 Diop^2
C_L:	2.125 Diop^2	0	0	0	1.0 Diop^2
D:	14.986 (.590)	9.525 (.375)	9.525 (.375)	9.525 (.375)	14.986 (.590)
E:	1.151 (.0453)	.429 (.0169)	.513 (.0202)	0.363 (.0143)	.386 (.0152)
FxG:	.635(.025)x30 Diop^2	.254(.010)x20 Diop^2	.254(.010)x20 Diop^2	.762(.030)x12 Diop^2	.762(.030)x20 Diop^2

1. L.P.D. = low profile diamond notch.
2. Diop = diopter: 1 Diop = Radius of curvature of 529.996 (20.866)
   2 Diop = Radius of curvature of 264.998 (10.433)

TYPICAL SC CUT DESIGNS

*A 5.115 MHz Fifth Overtone Crystal was also manufactured. All dimensions are the same except for A = 1.814 (.0714) and E = 1.100 (.0433).

FIGURE 2

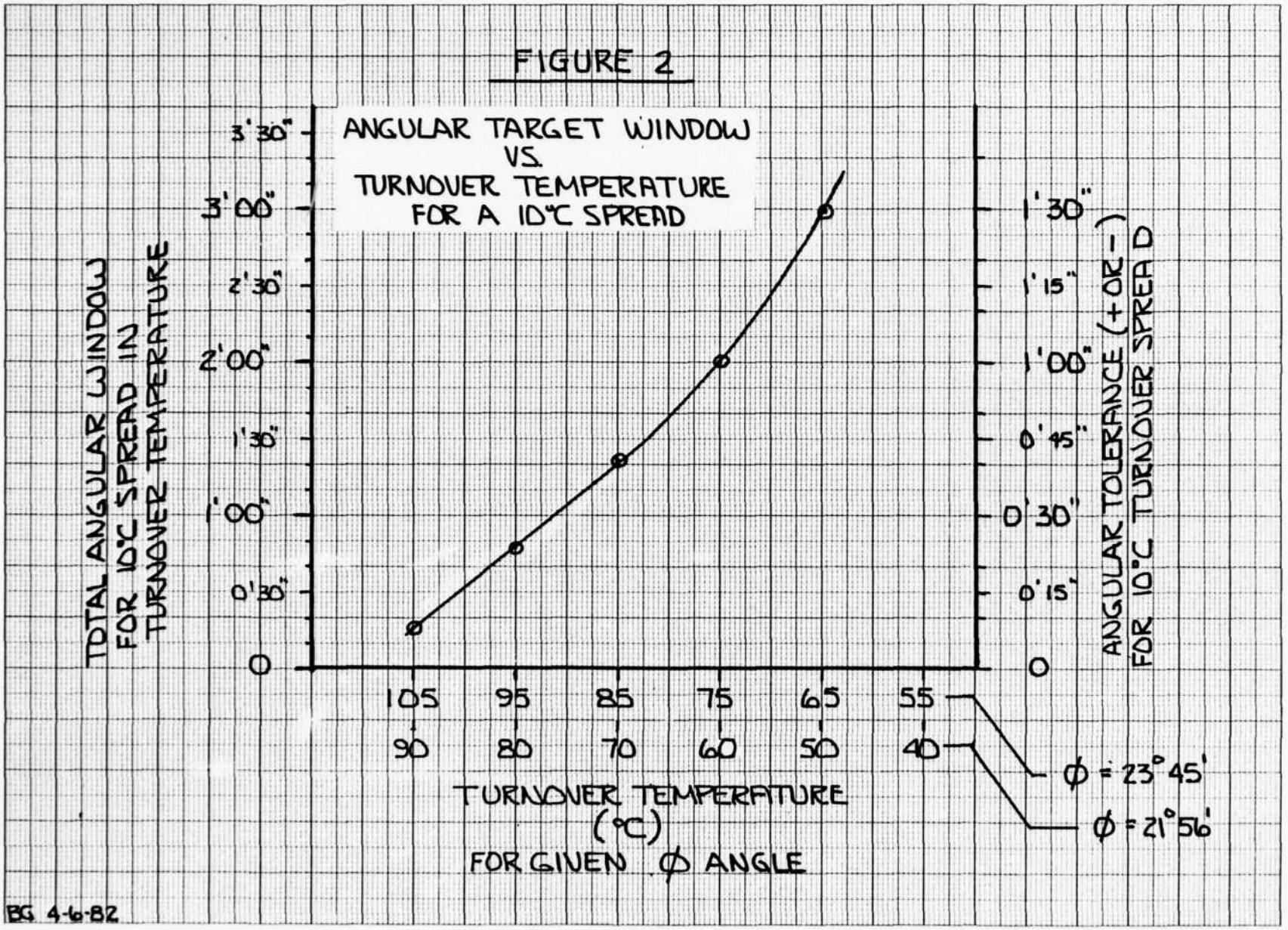

X-RAY GONIOMETER

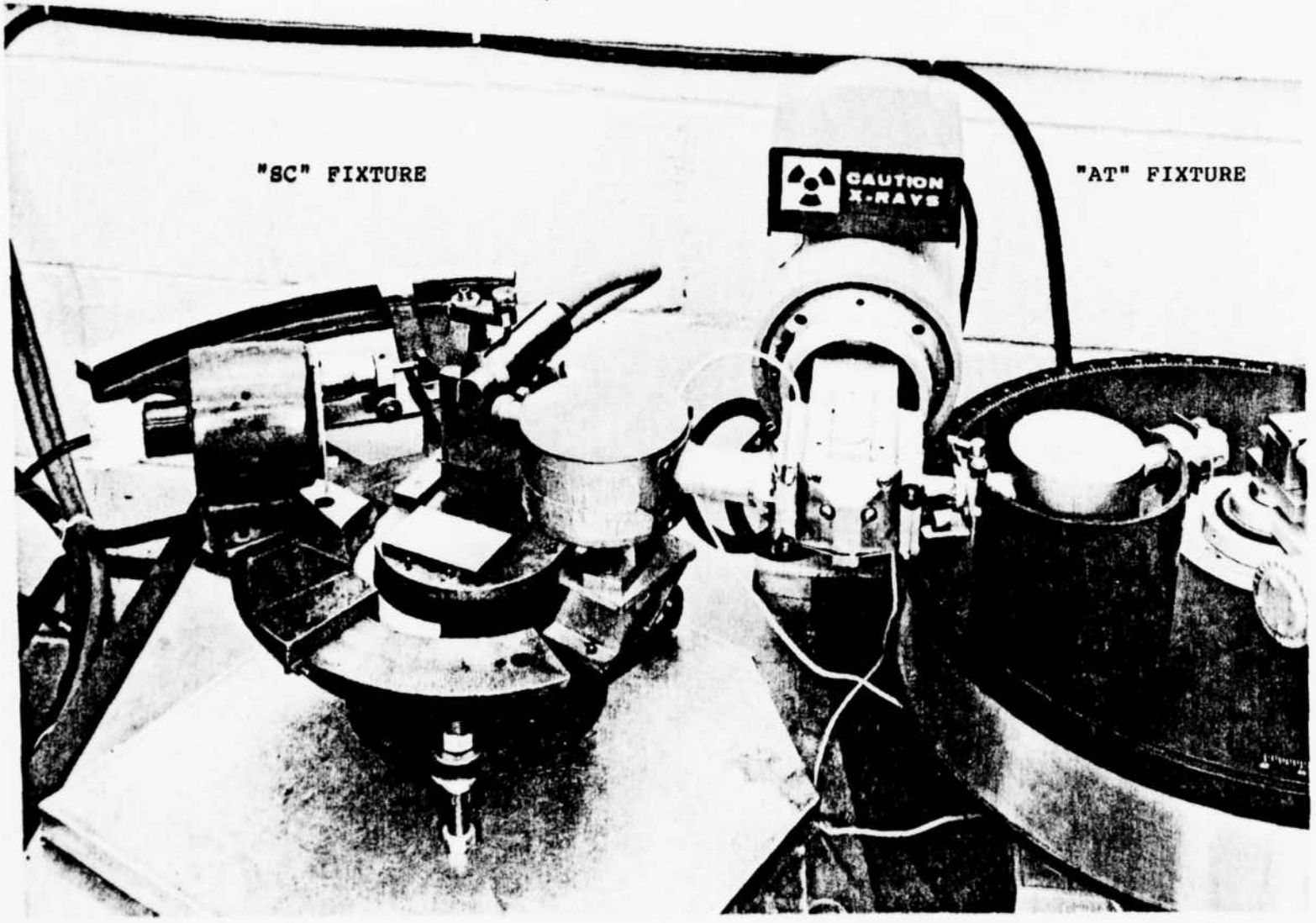

FIGURE 3

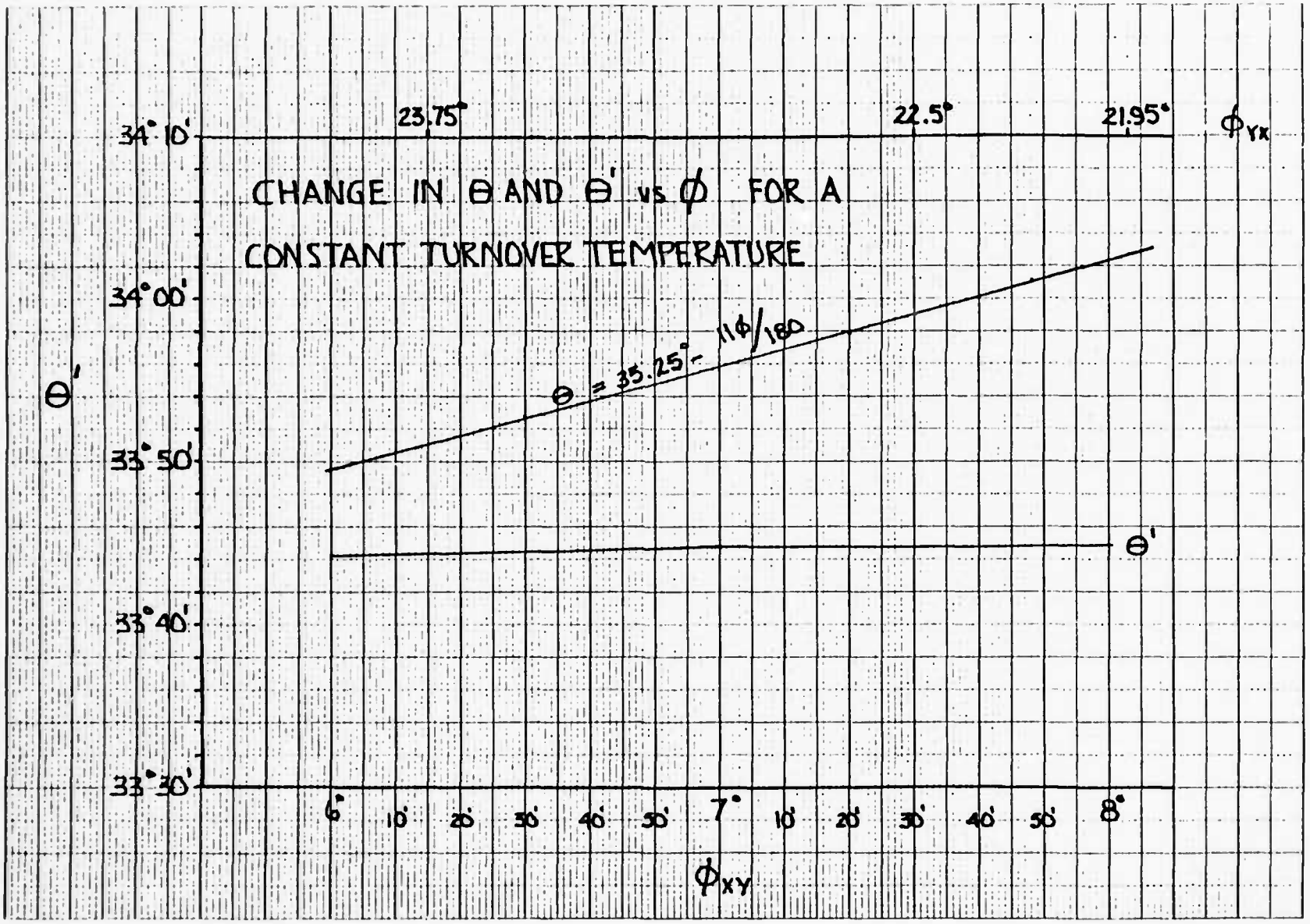
CHANGE IN Θ AND Θ' vs Φ FOR A CONSTANT TURNOVER TEMPERATURE
23.75°
22.5°
21.95°
Φ_{YX}
34° 10'
34° 00'
33° 50'
33° 40'
33° 30'
Θ'
Θ = 35.25° - 11Φ/180
Θ'
6°
10'
20'
30'
40'
50'
7°
10'
20'
30'
40'
50'
8°
Φ_{XY}

FIGURE 4

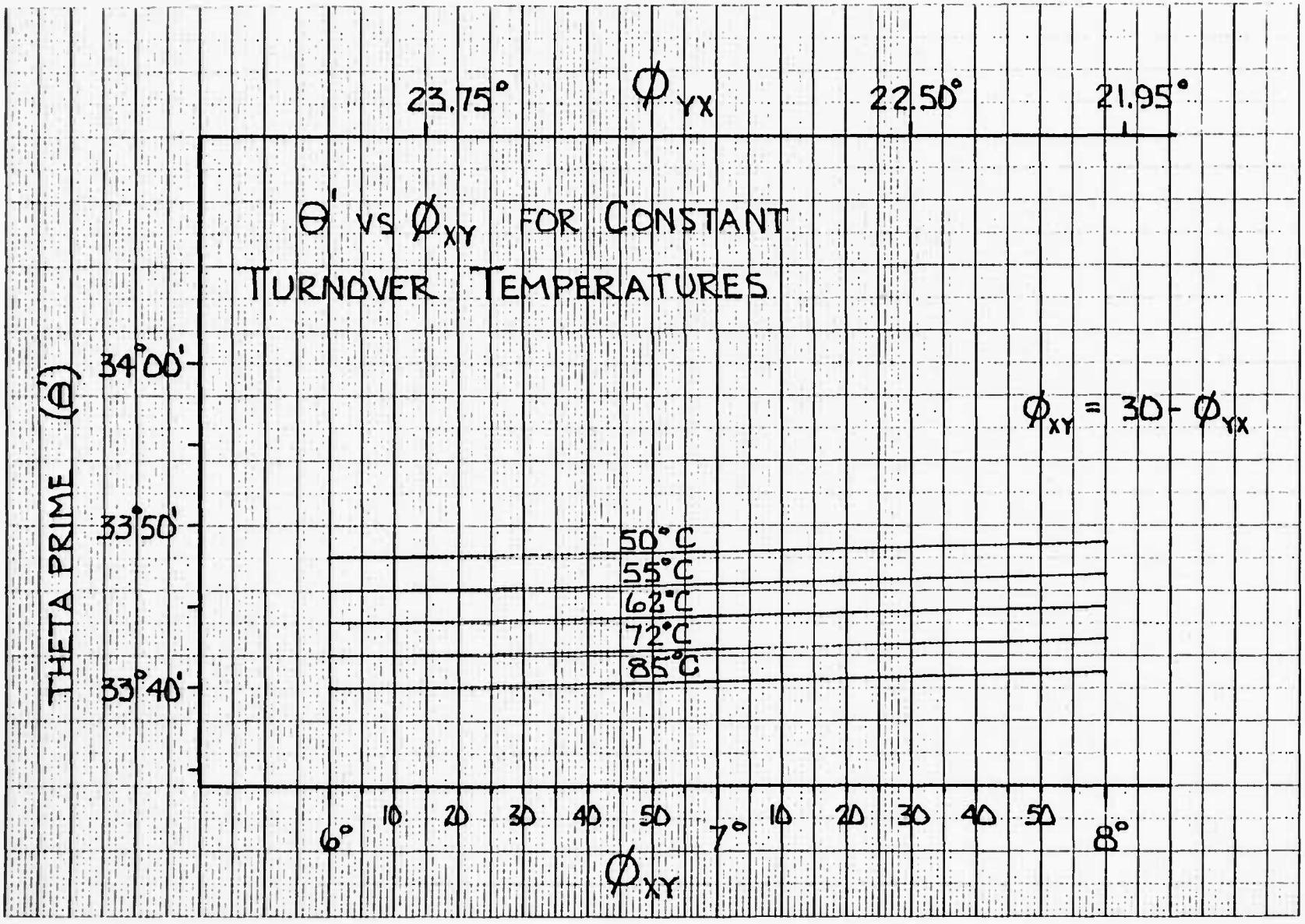
23.75°
ϕ_{YX}
22.50°
21.95°
θ' VS ϕ_{XY} FOR CONSTANT
TURNOVER TEMPERATURES
$\phi_{XY} = 30 - \phi_{YX}$
THETA PRIME (θ')
34°00'
33°50'
33°40'
50°C
55°C
62°C
72°C
85°C
6° 10 20 30 40 50 7° 10 20 30 40 50 8°
ϕ_{XY}

FIGURE 5

FIGURE 6

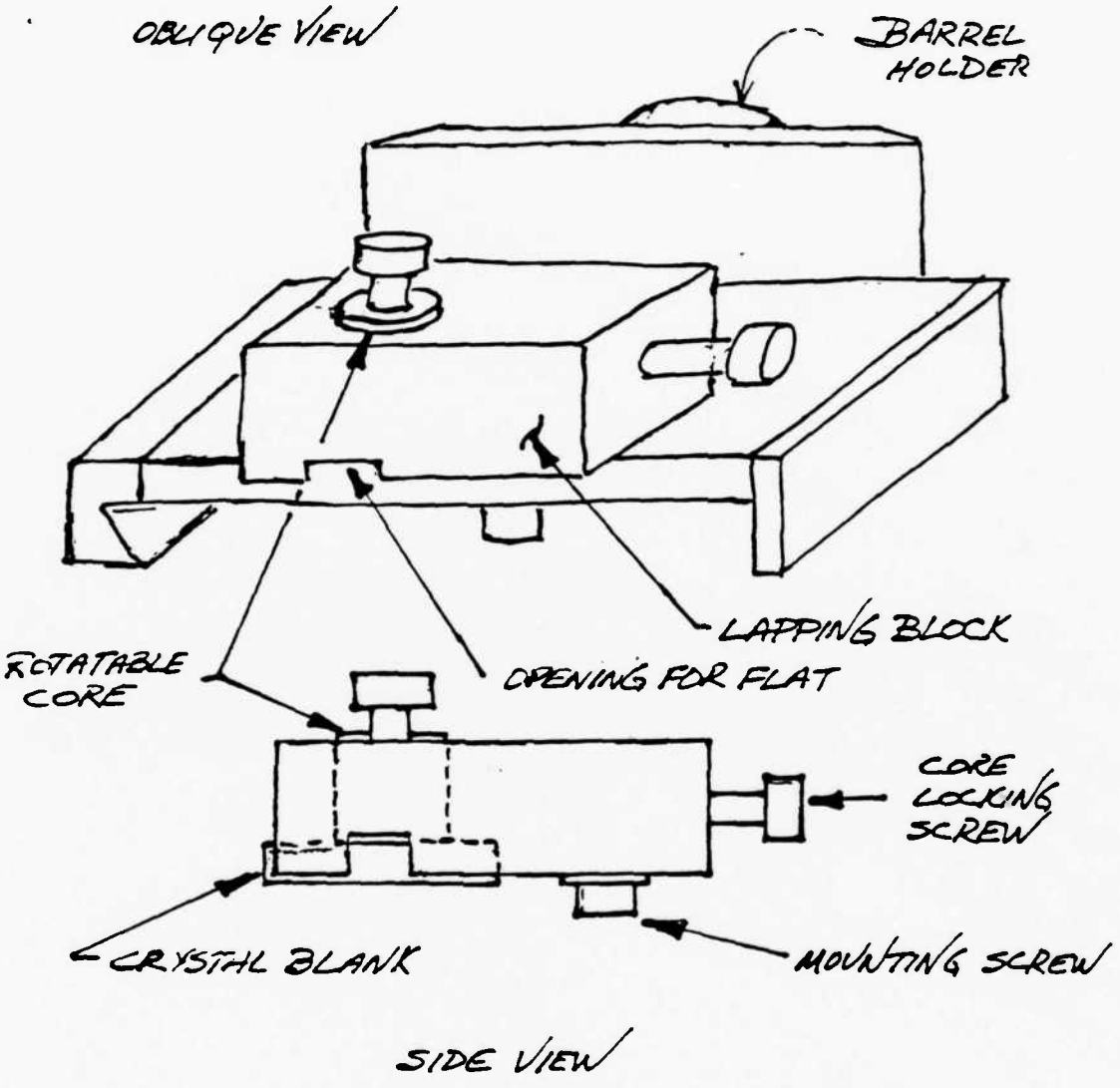

APPARATUS FOR LOCATING CRYSTAL BLANK MOUNTING FLATS

1. Lapping block is mounted on an adjustable barrel holder in the X-ray.

2. Crystal blank is waxed to the rotatable core.

3. By using the X-ray goniometer table and alternately using the core locking screws, the crystal blank is positioned correctly in the lapping blocks and locked.

4. Lapping block is removed from the X-ray and crystal flats generated by lapping.

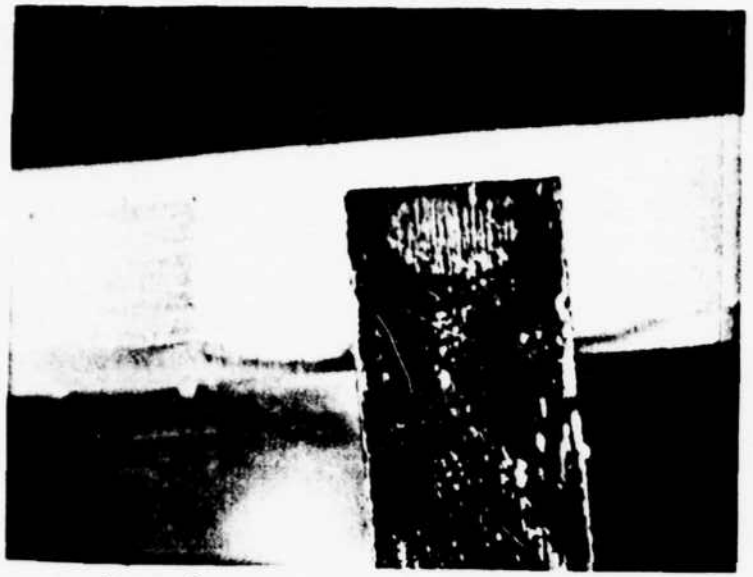

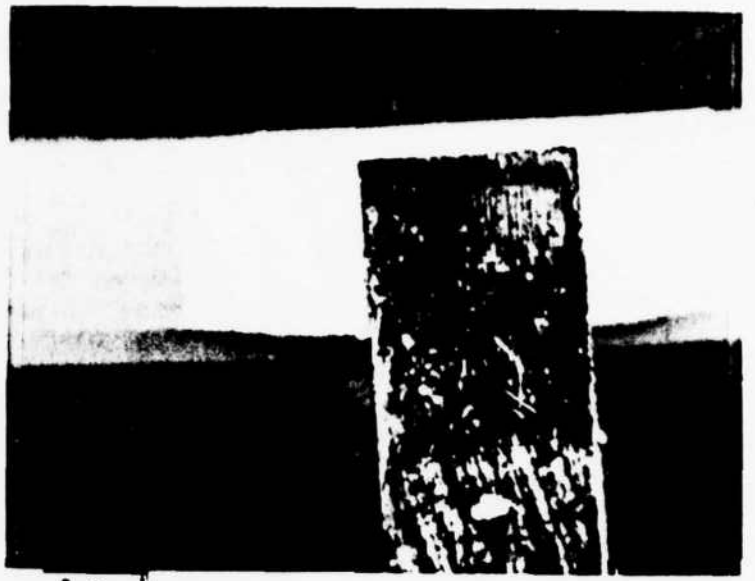

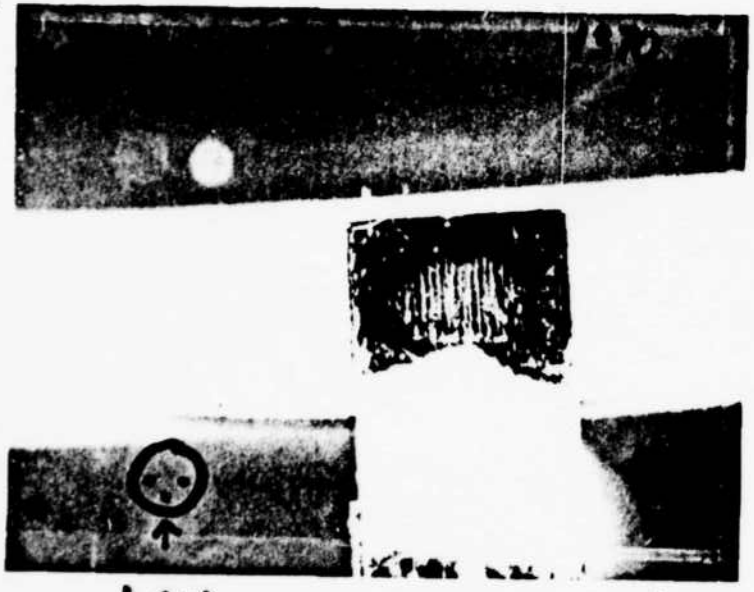

FIGURE 7

Nonactive bond well located. Both active bonds slightly high. One active bond toward right side of flat.

FIGURE 8

Nonactive bond high and to right. Active bonds high, and one slightly to right. One ribbon has excess material above crystal flat.

FIGURE 9

Nonactive bond and one active bond are high other active bond is centrally located. Small kink in active bond that is high.

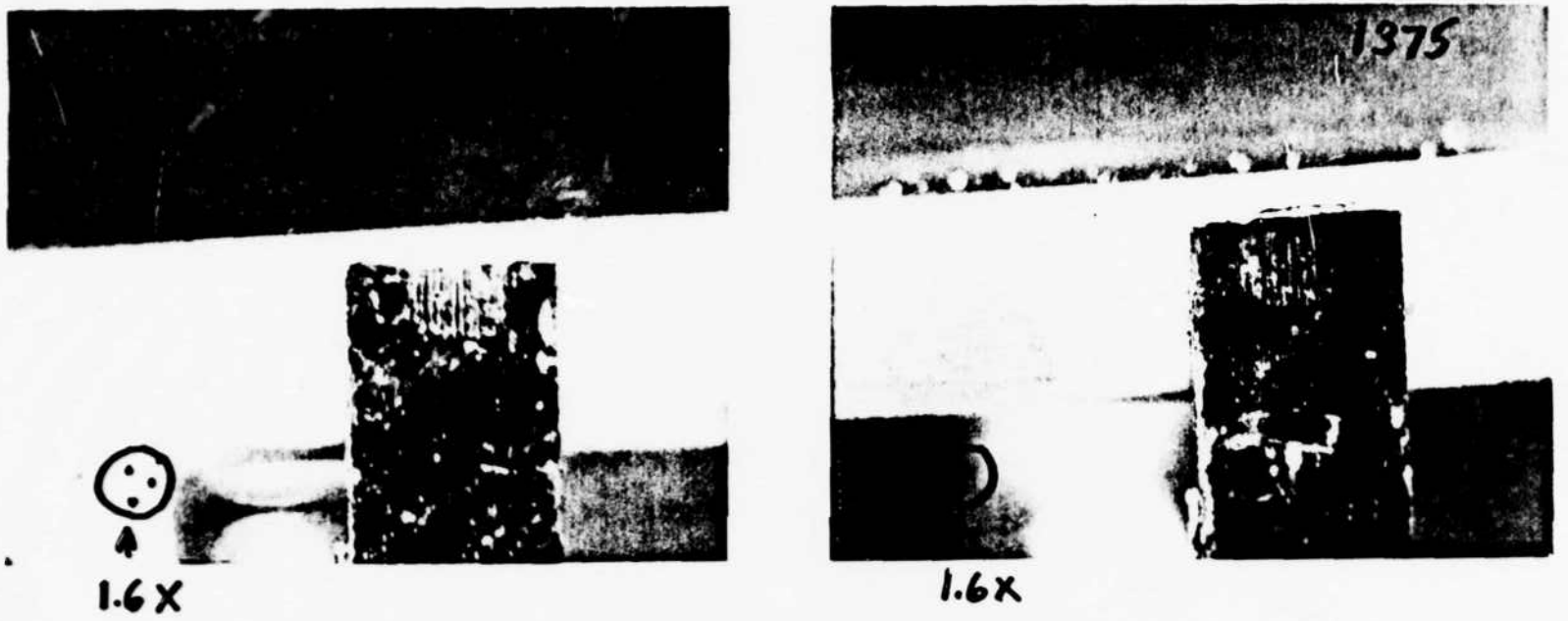

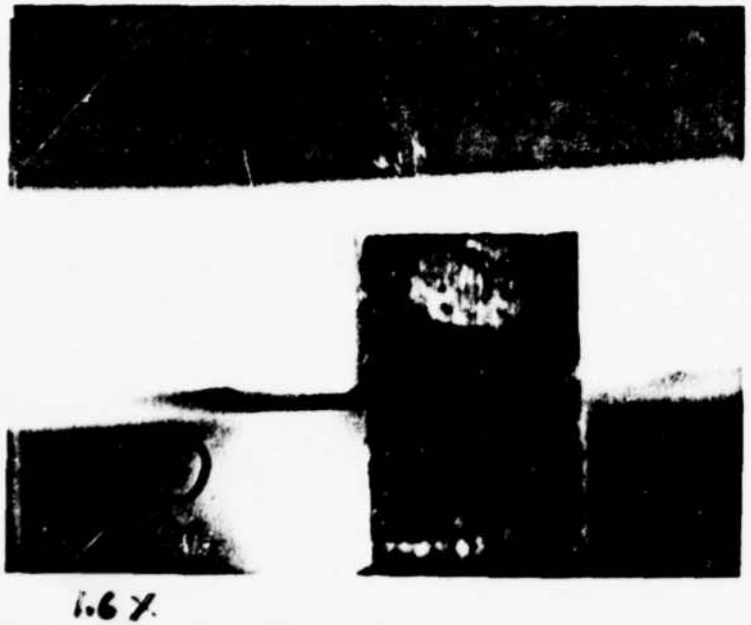

FIGURE 10

All bonds are high. One active bond partially off ribbon. Other active bond has slight kink in ribbon.

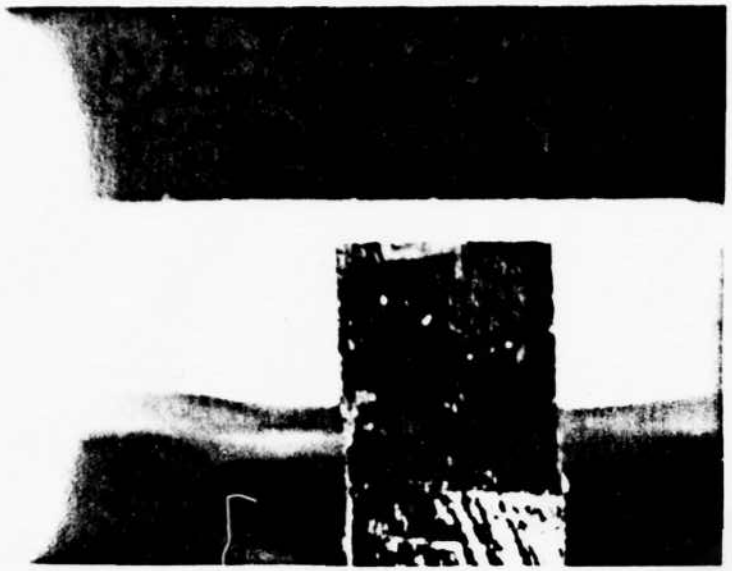

1.6X

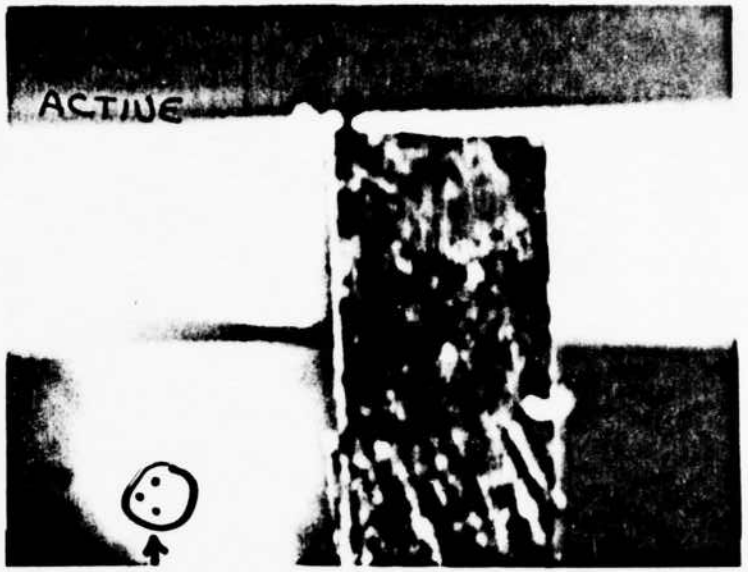

1.6X

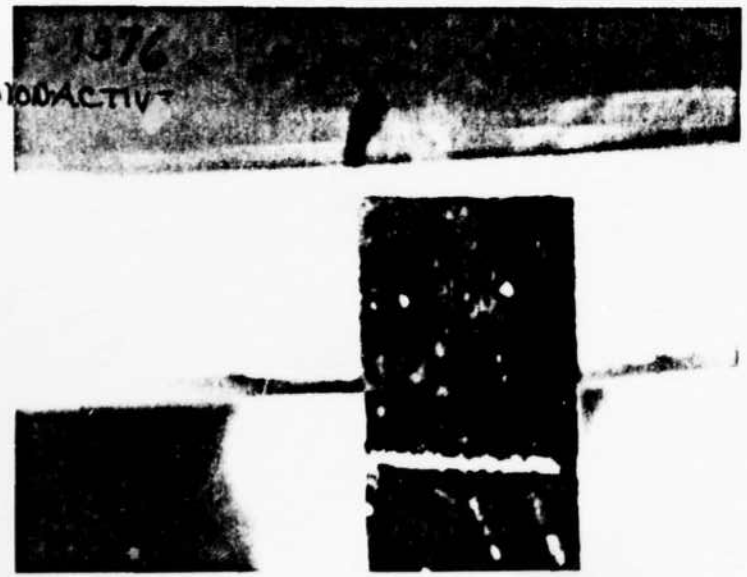

1.6X

FIGURE 11

All bonds slightly high. One active bond slightly to right. Excess ribbon on one active bond.

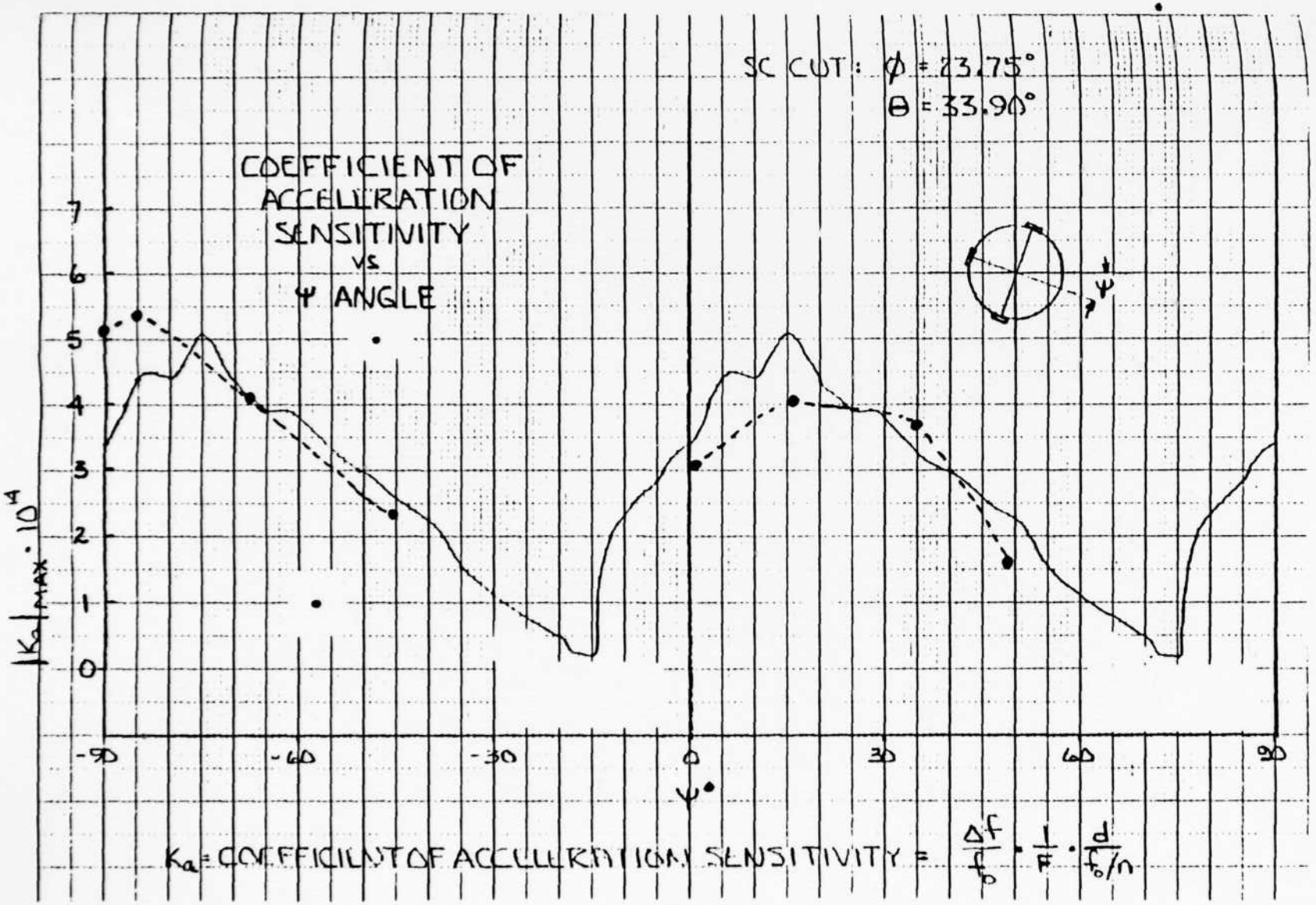

FIGURE 12

THEORETICAL AND EXPERIMENTAL PSI (ψ) ANGLES VS. ACCELERATION SENSITIVITY

FIGURE 13

PULL OFF PATTERNS FOR VERTICAL THERMOCOMPRESSION BONDS

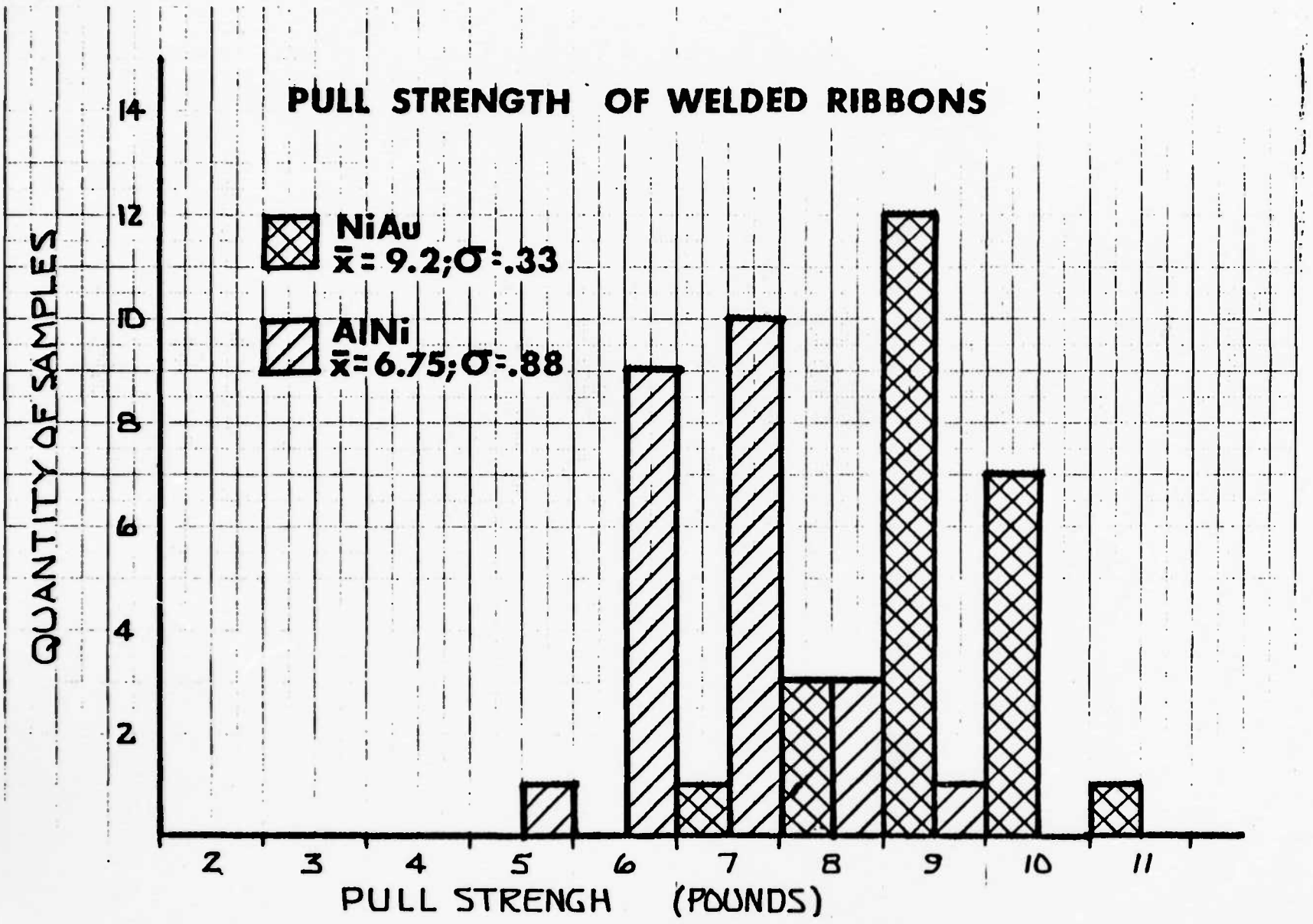
PULL STRENGTH OF WELDED RIBBONS
NiAu
x̄ = 9.2; σ = .33
AlNi
x̄ = 6.75; σ = .88
QUANTITY OF SAMPLES
14
12
10
8
6
4
2
2
3
4
5
6
7
8
9
10
11
PULL STRENGH (POUNDS)

FIGURE 14

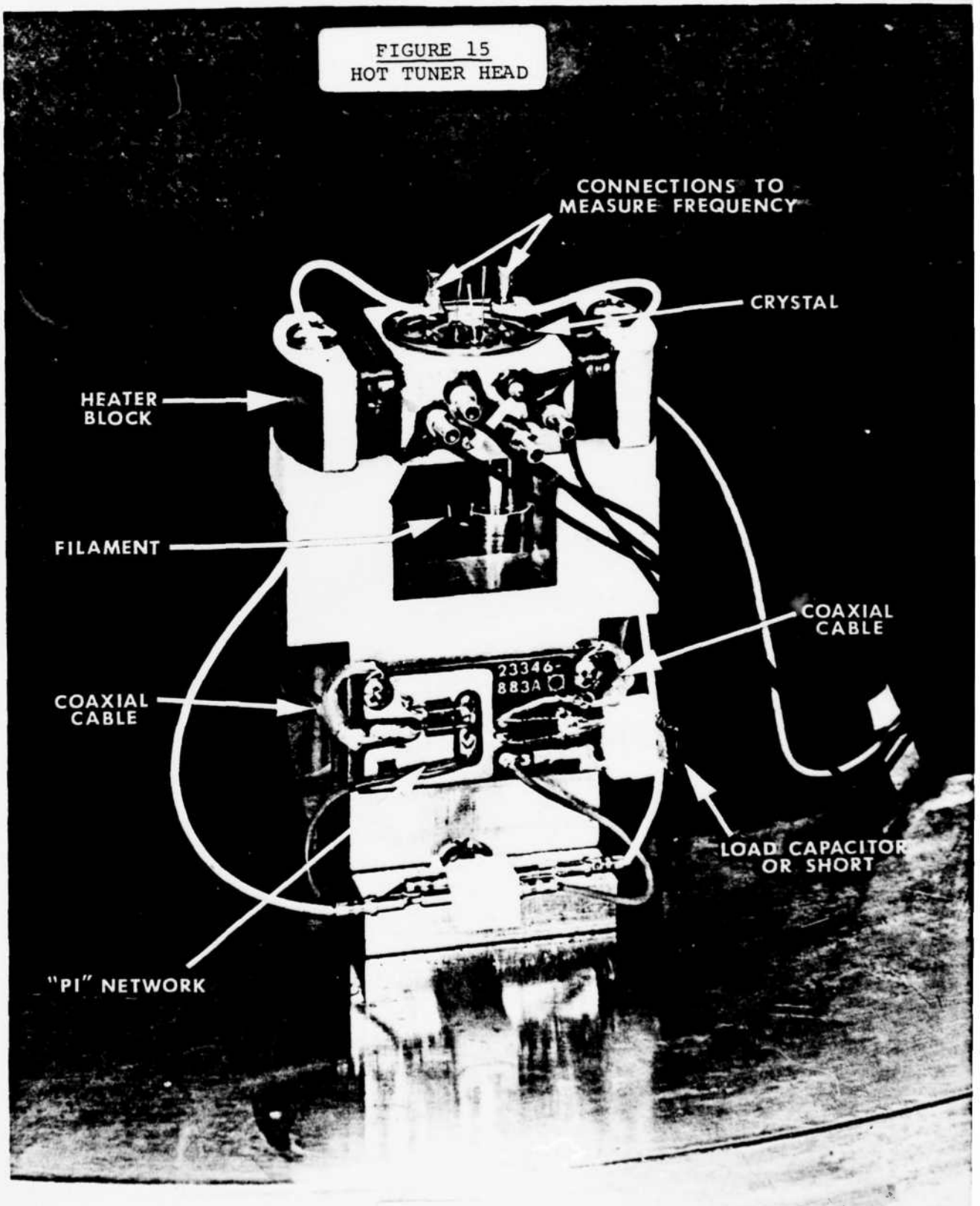
FIGURE 15
HOT TUNER HEAD
CONNECTIONS TO MEASURE FREQUENCY
CRYSTAL
HEATER BLOCK
FILAMENT
COAXIAL CABLE
23346-883A
COAXIAL CABLE
LOAD CAPACITOR OR SHORT
"PI" NETWORK

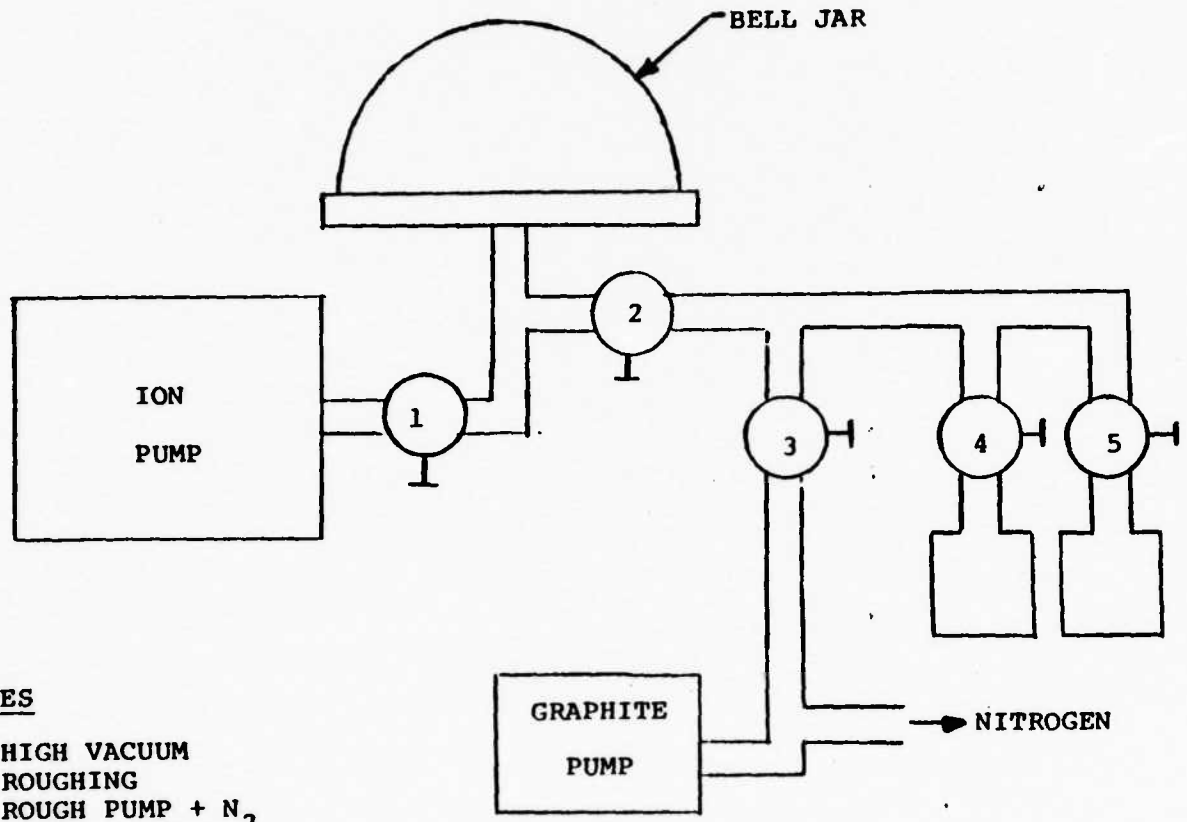

VALVES

1 - HIGH VACUUM
2 - ROUGHING
3 - ROUGH PUMP + N_2
4 & 5 - VAC-SORB PUMPS

FIGURE 16

HOT TUNER LAYOUT

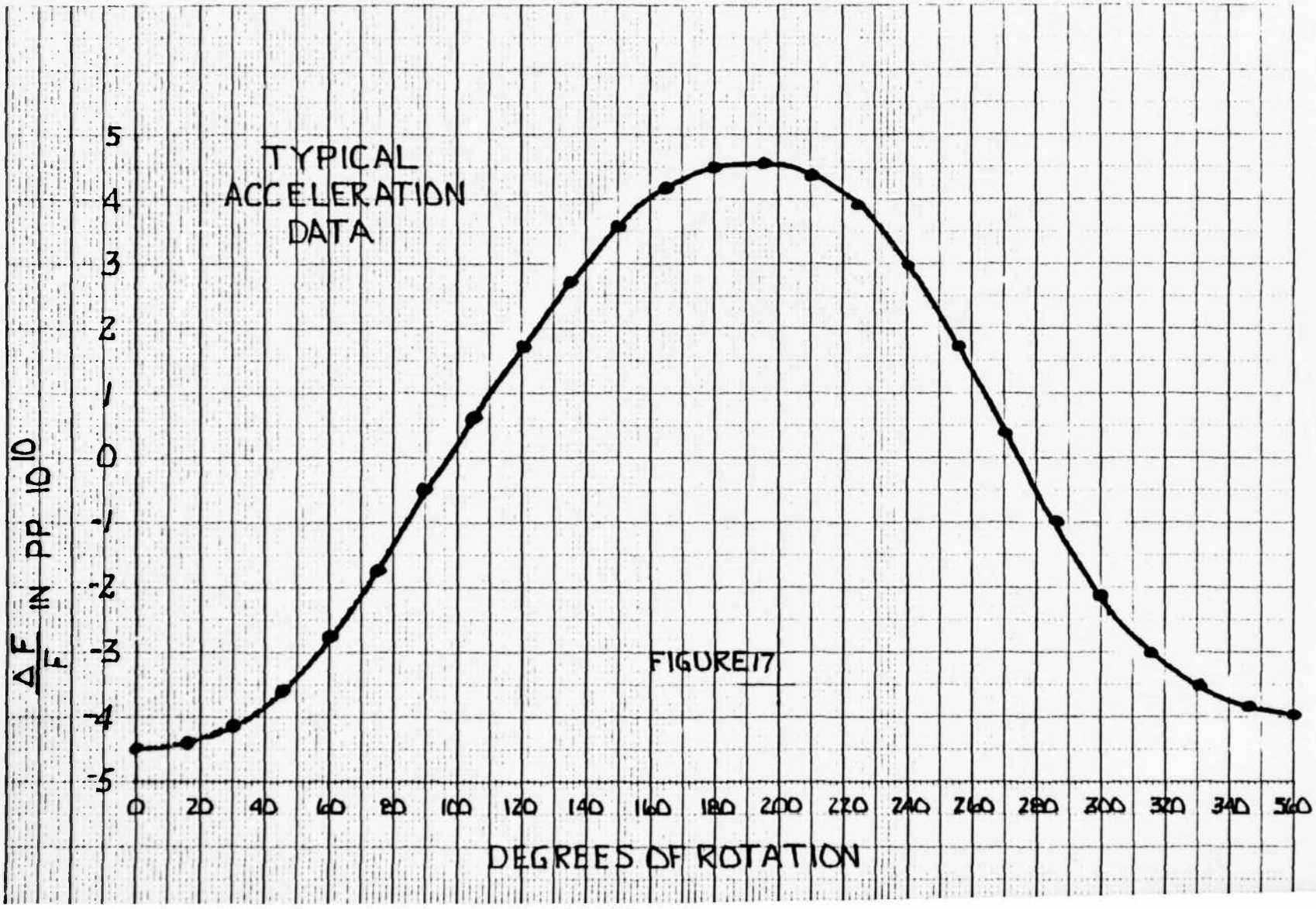
TYPICAL
ACCELERATION
DATA
$\frac{\Delta F}{F}$ IN PP 10^{10}
5
4
3
2
1
0
-1
-2
-3
-4
-5
0
20
40
60
80
100
120
140
160
180
200
220
240
260
280
300
320
340
360
DEGREES OF ROTATION

FIGURE 17

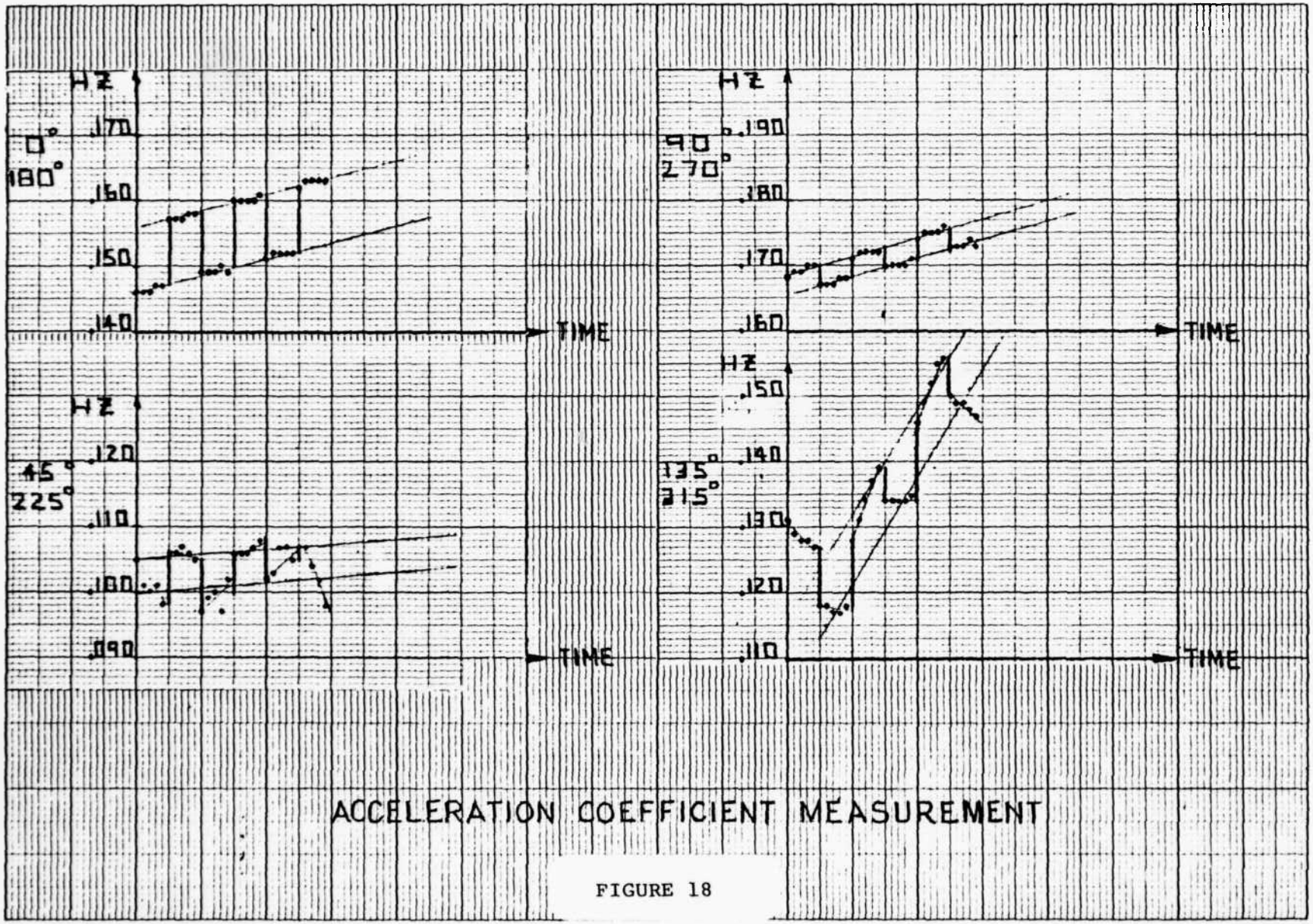

ACCELERATION COEFFICIENT MEASUREMENT

FIGURE 18

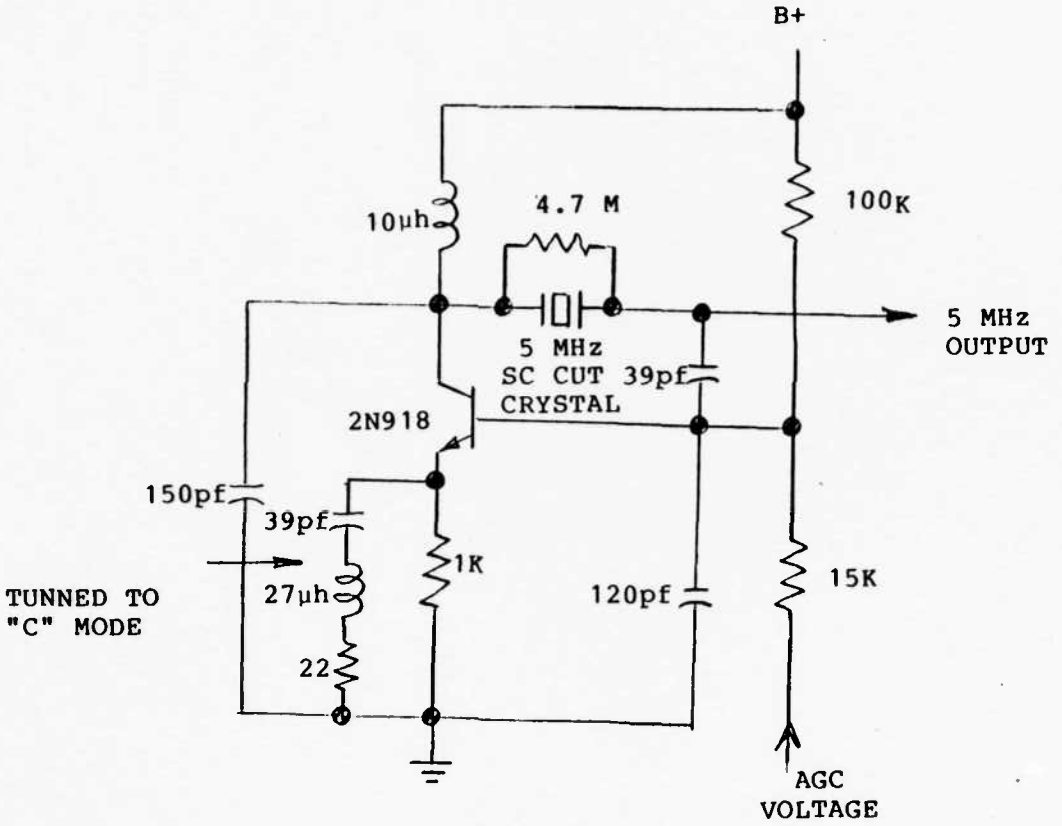

FIGURE 19

TYPICAL 5 MHz SC CUT 5th OVERTONE

OSCILLATOR CIRCUIT

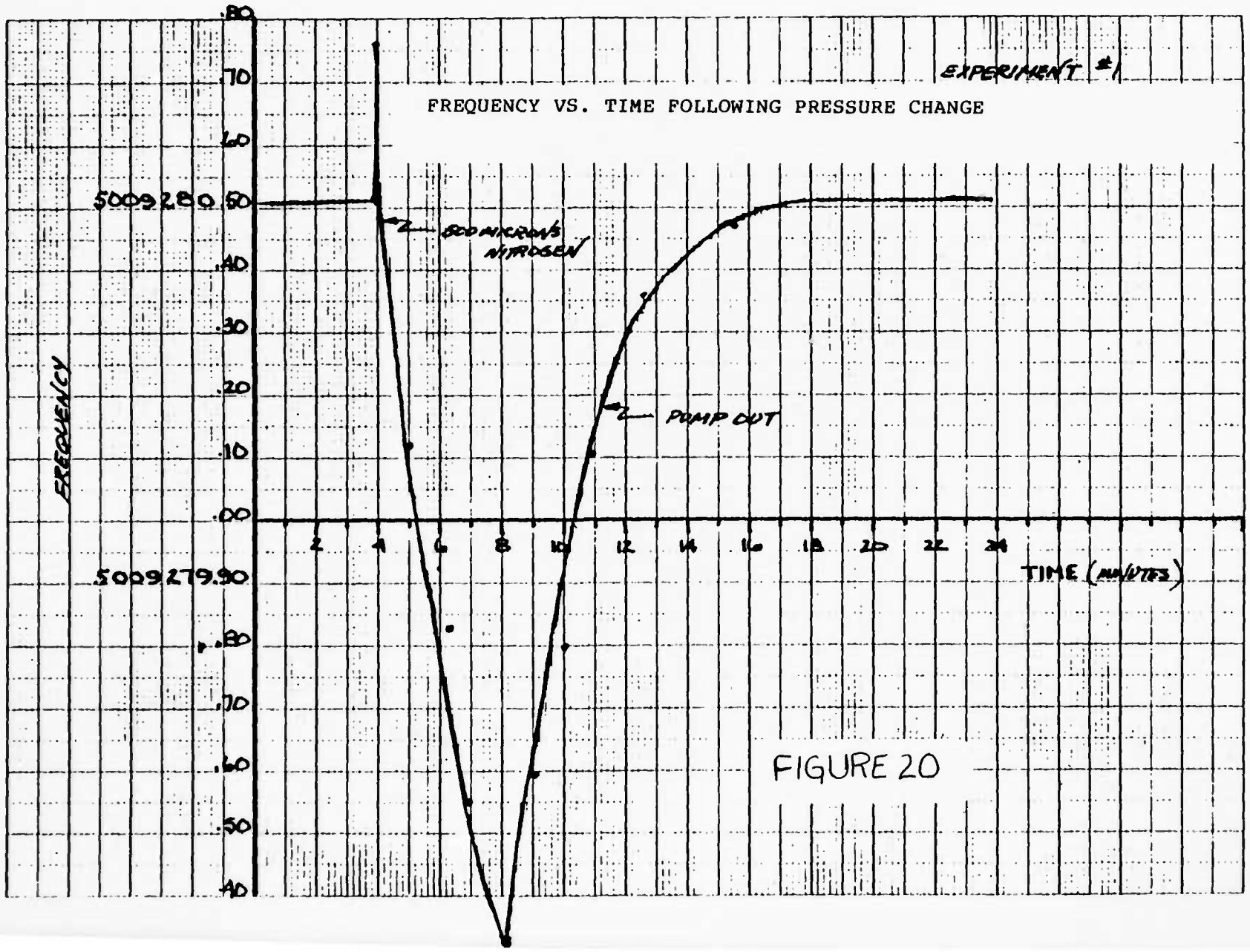
EXPERIMENT #1
FREQUENCY VS. TIME FOLLOWING PRESSURE CHANGE
500 MICRONS NITROGEN
PUMP OUT
FREQUENCY
5009280.60
5009279.90
.80
.70
.60
.50
.40
.30
.20
.10
.00
.80
.70
.60
.50
.40
2
4
6
8
10
12
14
16
18
20
22
24
TIME (MINUTES)

FIGURE 20

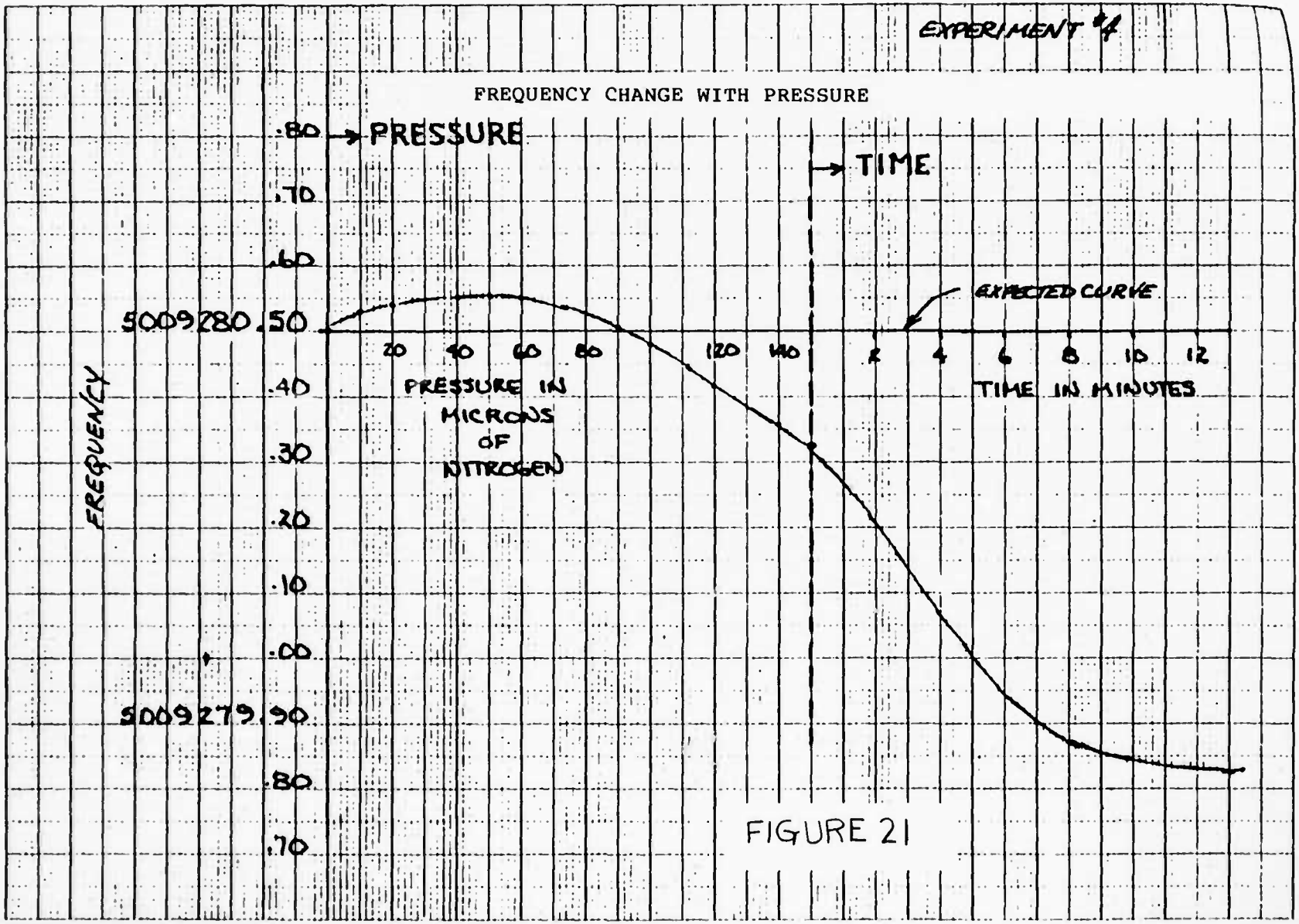
EXPERIMENT #4
FREQUENCY CHANGE WITH PRESSURE
PRESSURE
TIME
EXPECTED CURVE
5009280.50
5009279.90
FREQUENCY
.80
.70
.60
.40
.30
.20
.10
.00
.80
.70
20
40
60
80
120
140
2
4
6
8
10
12
PRESSURE IN MICRONS OF NITROGEN
TIME IN MINUTES

FIGURE 21

NUMBER OF UNITS	SHAPING	ϕ ANGLE	ψ ANGLE	RADIAL COMPONENT OF $\lvert\vec{\Gamma}\rvert$, $10^{-10}/g$		THICKNESS COMPONENT OF $\lvert\vec{\Gamma}\rvert$, $10^{-10}/g$		$\lvert\vec{\Gamma}\rvert$
				$\bar{x}$	Sx	$\bar{x}$	Sx	$10^{-10}/g$
5	PLANO-CONVEX (4 1/8 DIOPTER)	22.5°	-13.8°	6.0	2.2	3.0	1.7	6.7
7	PLANO-CONVEX (4 1/8 DIOPTER)	21.95°	-13.8°	4.3	2.3	2.5	1.0	5.0
3	DOUBLE-CONVEX (2 1/8 DIOPTER)	23.75°	-16.0°	2.6	1.16	.67	0.40	2.7
3	DOUBLE-CONVEX (2 1/8 DIOPTER)	21.95°	-17.0°	3.2	1.67	.80	0.46	3.3

FIGURE 22

AVERAGE VALUE AND STANDARD DEVIATION OF THE MAGNITUDE
OF THE ACCELERATION SENSITIVITY VECTOR OF 5 MHz, 5TH OVERTONE
PLANO-CONVEX AND DOUBLE-CONVEX CRYSTAL UNITS.

SERIAL NO.	ϕ ANGLE	ψ ANGLE	$\bar{\Gamma}_R$	RADIAL	$\bar{\Gamma}_T$	ϑ	$\lvert\vec{\Gamma}\rvert$
7006	21.93°	-27°	9.6	74°	1.2	7°	9.7
7008	22.28°	-27°	8.2	66°	0.7	5°	8.2
7009	22.04°	-25°	6.6	66°	0.8	7°	6.6
7010	22.17°	-25°	10.3	80°	1.7	9°	10.4
7011	22.35°	-23°	6.6	87°	0.4	3°	6.6
7012	22.30°	-23°	5.7	32°	1.4	14°	5.8

FIGURE 23

RADIAL COMPONENT, THICKNESS COMPONENT, AND MAGNITUDE OF THE ACCELERATION SENSITIVITY VECTOR, IN $PP10^{10}/g$ FOR 5 MHz, 5TH OVERTONE, 2 1/8 DIOPTER PER SIDE, BI-CONVEX CRYSTAL UNITS $\phi = 22°$, ψ NEAR -25°

#	ψ	ϕ	R_1 OHMS	°C TURNOVER TEMP.	$\lvert\vec{\Gamma}\rvert$ $10^{-10}/g$
1A	+7°	21.6°	270	37	10
2A	+4°	22.0°	260	41	9
3A	+4°	22.3°	275	37	8
4A	+5°	22.1°	280	50	5
1B	N O T	S E A L E D			
2B	-4°	22.0°	1000+	44	
3B	-6°	N O T	T E S T E D		8
4B	-4°	21.9°	900	46	
1C	-11°	22.1°	325	48	5
2C	-11°	22.2°	290	45	5
3C	-11°	22.2°	270	50	5
4C	-11°	22.1°	300	50	5
1D	-17°	22.0°	300	50	4
2D	-15°	N O T	T E S T E D		3
3D	-16°	22.3°	270	50	3
4D	-15°	22.0°	260	40	16
1E	-20°	N O T	T E S T E D		5
2E	-20°	22.1°	260	50	14
3E	-20°	21.9°	300	46	10
4E	-20°	22.1°	350	37	10

FIGURE 24

MAGNITUDE OF THE ACCELERATION SENSITIVITY VECTOR VS. ψ ANGLE, 5 MHz, 5TH OVERTONE

#	Γ_X	Γ_Y	Γ_Z	$\lvert\vec{\Gamma}\rvert$	∠ RADIAL	∠ THICKNESS	QUARTZ PLATE MOUNTING: ∠ SPREAD 90° FLATS	TC BOND LOCATION	Ψ ANGLE
A1	-10	1	+3	10.5	16°	5°	1°		+7°
2	-7	1	-5	8.6	35°	7°	0	C LOW	+4°
3	+7	1	2	7.3	16°	8°	3°		+4°
4	5	1	1.5	5.3	17°	11°	1°	B LOW	+5°
B1	(NOT SEALED)								
2	(HIGH R)			N O T T E S T E D			1°		-4°
3	8		-3	8.6	20°		1°	B LOW, A RIGHT	-6°
4	←		B R O K E N	→			0		-4°
C1	4	0	-2	4.5	27°	0	0	ALL LEFT, B HIGH	-11°
2	5		1.5	5.2	17°		0	A HIGH, BE LEFT, C HIGH	-11°
3	-3	2	2	4.1	34°	29°	1°	A AND B LOW	-11°
4	4.5	2	1	5	12°	23°	1°	A LOW, C LOW AND RIGHT	-11°
D1	0	2	-3	3.6	90°	34°	2°	A LOW	-17°
2	-1.5	2	1	2.7	53°	39°	1°	B RIGHT	-15°
3	3		-2	3.6	34°		1°	B LOW, C HIGH	-16°
4	9	1	-13	16	55°	4°	2°	A LOW, B HIGH, C HIGH	-15°
E1	-4	0	4	5.6	45°	0	1°	B HIGH	-20°
2	.5	1	14	14	88°	4°	3°	C LEFT	-20°
3	5	1	-9	10.3	61°	6°	1°	B LEFT, C HIGH	-20°
4	-10	0	0	10	0	0	1°	A AND B HIGH, C LOW	-20°

FIGURE 25

ORTHOGONAL COMPONENTS OF THE ACCELERATION SENSITIVITY VECTOR VS. MOUNTING FOR 5 MHz, 5TH OVERTONE, BI-CONVEX CRYSTALS

FIGURE 26

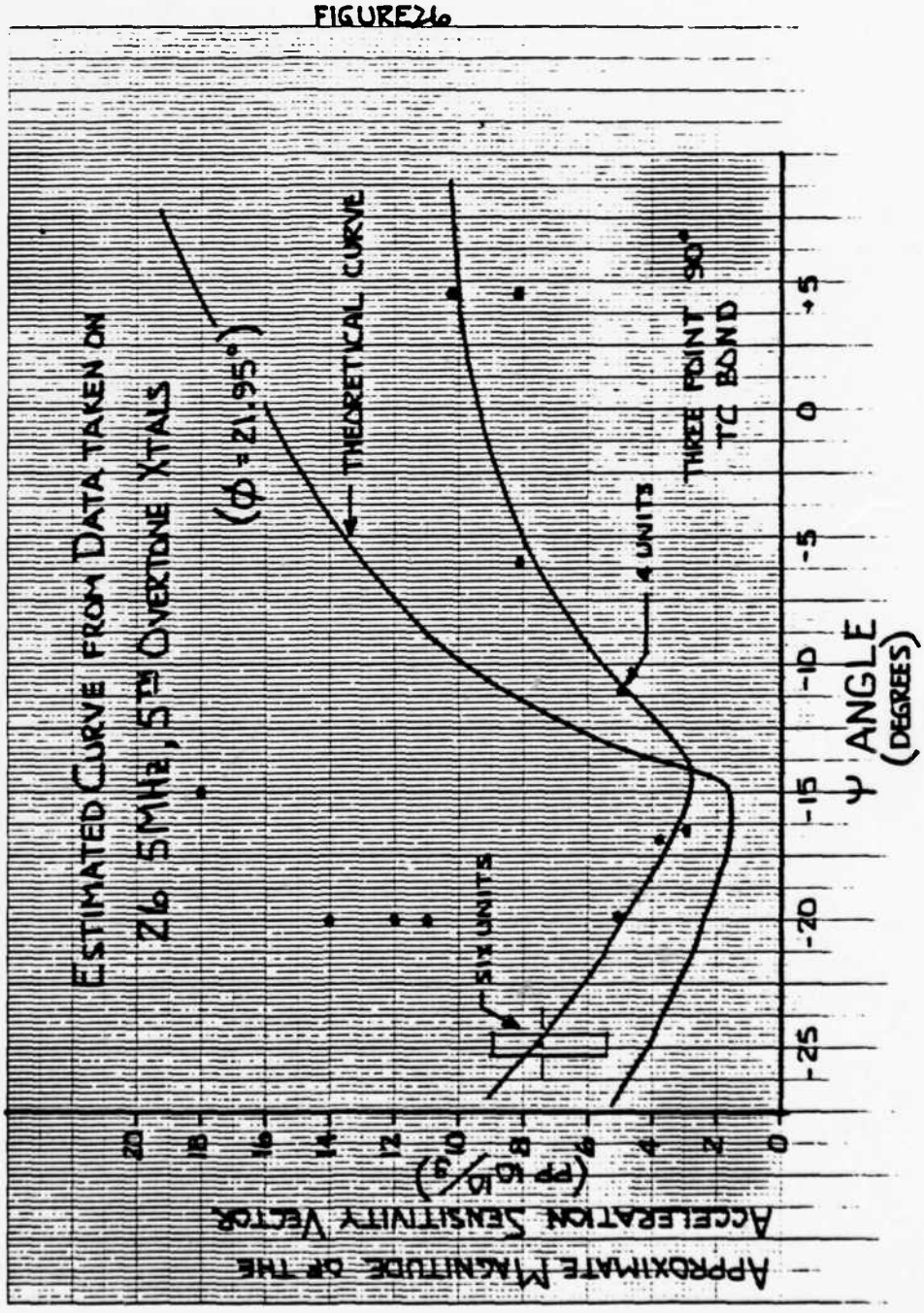
ESTIMATED CURVE FROM DATA TAKEN ON
26.5 MHz, 5TH OVERTONE XTALS
(Φ = 21.95°)
THEORETICAL CURVE
4 UNITS
THREE POINT 90°
TC BOND
SIX UNITS
APPROXIMATE MAGNITUDE OF THE
ACCELERATION SENSITIVITY VECTOR
(PPB/G)
ψ ANGLE
(DEGREES)
20
18
16
14
12
10
8
6
4
2
0
+5
0
-5
-10
-15
-20
-25

GROUP	SERNO	ψ	ϕ	INITIAL DATA			REPROCESSED DATA		
				RESISTANCE (Ω)	$T_{T.O.}$ (°C)	Γ_{Al} ($\times 10^{-10}$)	Γ_{Au} ($\times 10^{-10}$)	R (Ω)	$T_{T.O.}$ (°C)
A	7416	7	21.6	270	37	10	2.5	40	225
	7417	4	22.0	260	41	9	5.5	44	270
	7418	4	22.3	275	37	8	5.6	41	270
	7419	5	22.1	280	50	5	19.0	50	300
B	7420	-	-	-	-	-	1.3	48	240
	7421	-4	22	1000	44	-	2.5	50	260
	7422	-6	-	-	-	8	3.5	48	310
	7423	-4	21.9	900	46	-	4	48	260
C	7424	-11	22.1	325	48	5	1.3	48	270
	7425	-11	22.2	290	45	5	3.7	50	260
	7426	-11	22.2	270	50	5	4.0	46	200
	7427	-11	22.1	300	50	5	9.0	-	200
D	7428	-17	22.0	300	50	4	9.5	49	200
	7429	-15	-	-	-	3	5	47	240
	7430	-16	22.3	270	50	3	4.5	40	300
	7431	-15	22.0	260	40	16	-	-	-
E	7432	-20	-	-	-	5	3	43	270
	7433	-20	22.1	260	50	14	4.2	39	220
	7434	-20	21.9	300	46	10	7.5	48	220
	7435	-20	22.1	350	37	10	13.5	50	220

FIGURE 27

SUMMARY OF "g" SENSITIVITY DATA FOR VARIOUS MOUNTING ANGLES (ψ)
OR 5 MHz, 5TH OVERTONE BI-CONVEX CRYSTALS

CRYSTAL SERNO	Γ 0° 180° x10^{-10}	Γ 45° 225° x10^{-10}	Γ 90° 270° x10^{-10}	Γ 135 315 x10^{-10}	UP DOWN x10^{-10}	$\vec{\Gamma}$ x10^{-10}	R_S (Ω)	Q x10^{-}
8145	1.2	4.2	3.0	1.4	5.0	6.0	750	1.3
8146	3.5	4.6	6.0	4.6	2.5	7.4	650	1.5
8147	-1.2	0.2	1.4	2.8	1.0	2.1	845	1.2
8149	5.3	1.2	-2.0	3.8	0	5.6	580	1.7
8150	-1.2	-2.0	-1.2	-0.2	-1.5	2.3	330	2.9
8151	-3.4	0	4.6	6.0	1.5	5.9	330	2.9
8152	-1.0	-0.2	-0.2	-0.2	1.0	1.4	350	2.8
8153	-1.0	0.7	0.4	0.2	-2.5	2.7	700	1.4
8156	0.8	1.4	0.4	-0.4	-0.5	1.0	500	2.0
8157	13.5	4.0	9.4	6.2	-3.5	16.8	330	2.9
8158	1.6	1.6	1.8	0.8	-1.0	2.6	350	2.8
9071	1.6	1.4	5.0	6.4	-1.0	5.3	-	-
9072	8.0	9.6	8.0	-4.0	-7.5	13.6	350	2.8
9073	1.0	1.2	0.3	0.6	-2.0	2.3	380	2.6
9074	2.2	1.8	-5.0	-5.3	-9.4	10.9	510	1.9
9075	1.0	2.6	1.6	1.0	-0.5	2.8	350	2.8
9076	4.4	2.5	-2.5	-	-1.0	5.2	480	2.0

$\vec{\Gamma}_{AV}$ (17 values) = 5.5

$\vec{\Gamma}_{AV}$ (14 values) = 3.8

σ_{17} = 4.5

σ_{14} = 2.0

FIGURE 28

ACCELERATION SENSITIVITY FOR ϕ = 25°

ON 5.115 MHz, 5TH OVERTONE SC CUT CRYSTALS

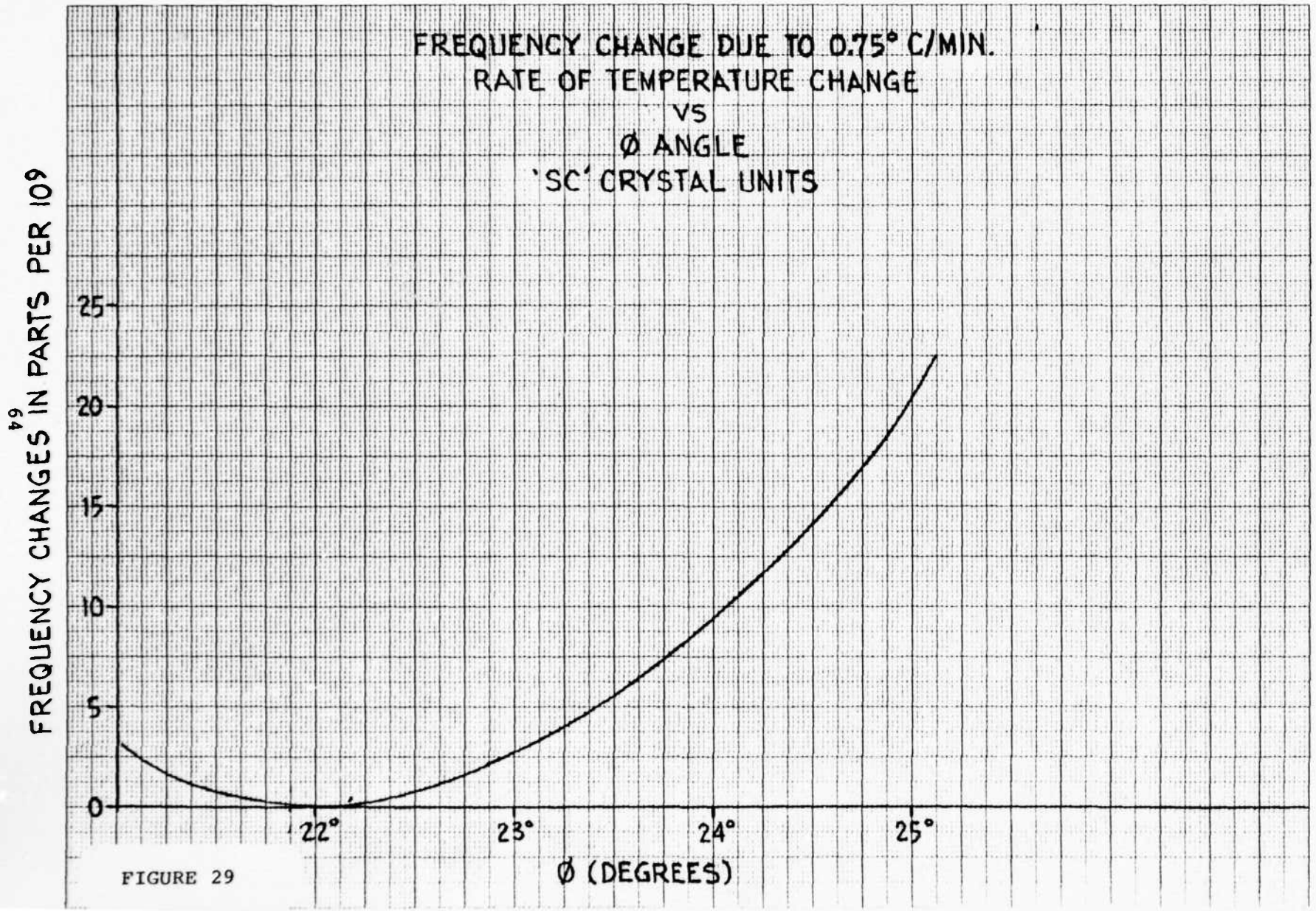

FIGURE 29

FREQUENCY vs CURRENT
FOR 'SC' CUT CRYSTALS WITH DIFFERENT ϕ ANGLES

CHANGE IN FREQUENCY (PP 10^9)

40
30
20
10
0
-10

.01ma .1ma 1ma

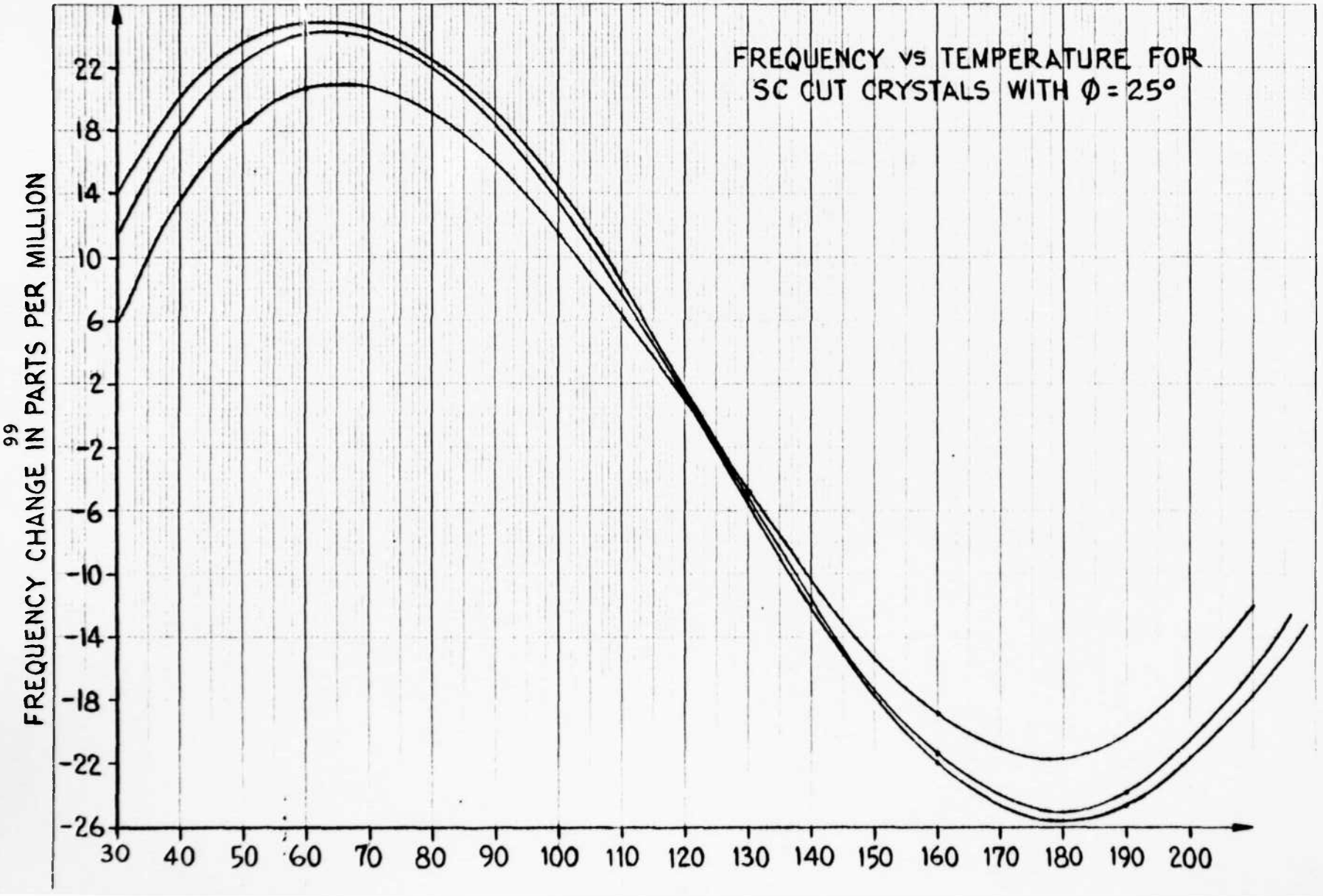
FREQUENCY vs TEMPERATURE FOR
SC CUT CRYSTALS WITH Ø = 25°
FREQUENCY CHANGE IN PARTS PER MILLION
99
22
18
14
10
6
2
-2
-6
-10
-14
-18
-22
-26
30
40
50
60
70
80
90
100
110
120
130
140
150
160
170
180
190
200

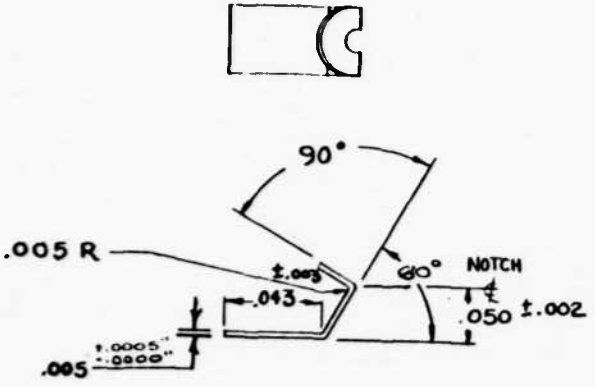

J MOUNT

INCHES	MM	INCHES	MM
.0005	.013	.043	1.092
.002	.051	.050	1.270
.003	.076	.065	1.651
.005	.127	.080	2.032
.015	.281	.090	2.286
.020	.508	.125	3.175
.040	1.016	.170	4.318

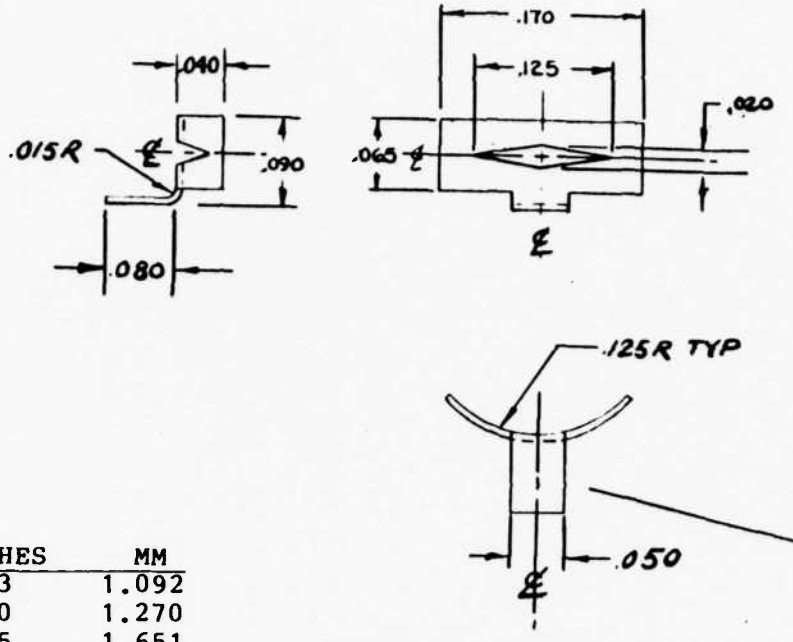

DIAMOND MOUNT

FIGURE 31A

TYPICAL MOUNTS USED ON 10.054 MHz, 3RD OVERTONE SC CUT CRYSTALS
(ALL DIMENSIONS IN INCHES)

FIGURE 32

ELECTRICAL TEST DATA

SERNO.	f_s @ 25°C	R	f_p @ 25°C w/32 pF	Δf	C_o	$C_1 \times 10^{16}$	Q x 10^{-6}	T.O.(°C)
3803	10.054200	80	10.054220	20	3.5	1.41	1.40	70
3804	10.054186	80	10.054206	20	3.5	1.41	1.40	64
3806	10.054176	80	10.054196	20	3.5	1.41	1.40	72
3807	10.054170	80	10.054190	20	3.5	1.41	1.40	72

ACCELERATION DATA

S/N	RADIAL WORST CASE ($PP10^{10}/g$)	THICKNESS (UP/DOWN) ($PP10^{10}/g$)	COMMENTS
3803	7.0	2.7	Diamond Mount
3804	5.3	3.0	Diamond Mount
3806	8.0	4.8	Diamond Mount
3807	2.7	2.5	Diamond Mount
3803	6.5	4.4	'J' Mount
3804	7.1	4.3	'J' Mount
3806	5.7	4.8	'J' Mount
3807	5.5	2.0	'J' Mount
3803	6.8	4.6	'J' Mount Retest
3804	6.7	4.2	'J' Mount Retest
3807	6.0	2.6	'J' Mount Retest

ELECTRICAL AND ACCELERATION DATA FOR 10.054 MHz, 3RD OVERTONE, PLANO CONVEX CRYSTALS

K·E 20 X 20 TO THE INCH • 7 X 10 INCHES KEUFFEL & ESSER CO MADE IN U.S.A.

SER NO. 4182 10.230400|3|SC DATE 9-5-80

FIGURE 33A

FREQUENCY CHANGE IN PPM

6 5 4 3 2 1 0 -1 -2 -3 -4 -5 -6

UP 10.595

DOWN 10.711

11.6 PP1010/2g

3.4 x 10^10/g

0° 90° 180° 270° 360°

ROTATION IN DEGREES

46 1240

SER NO. 4184 10.230400|3|SC DATE 9-5-80

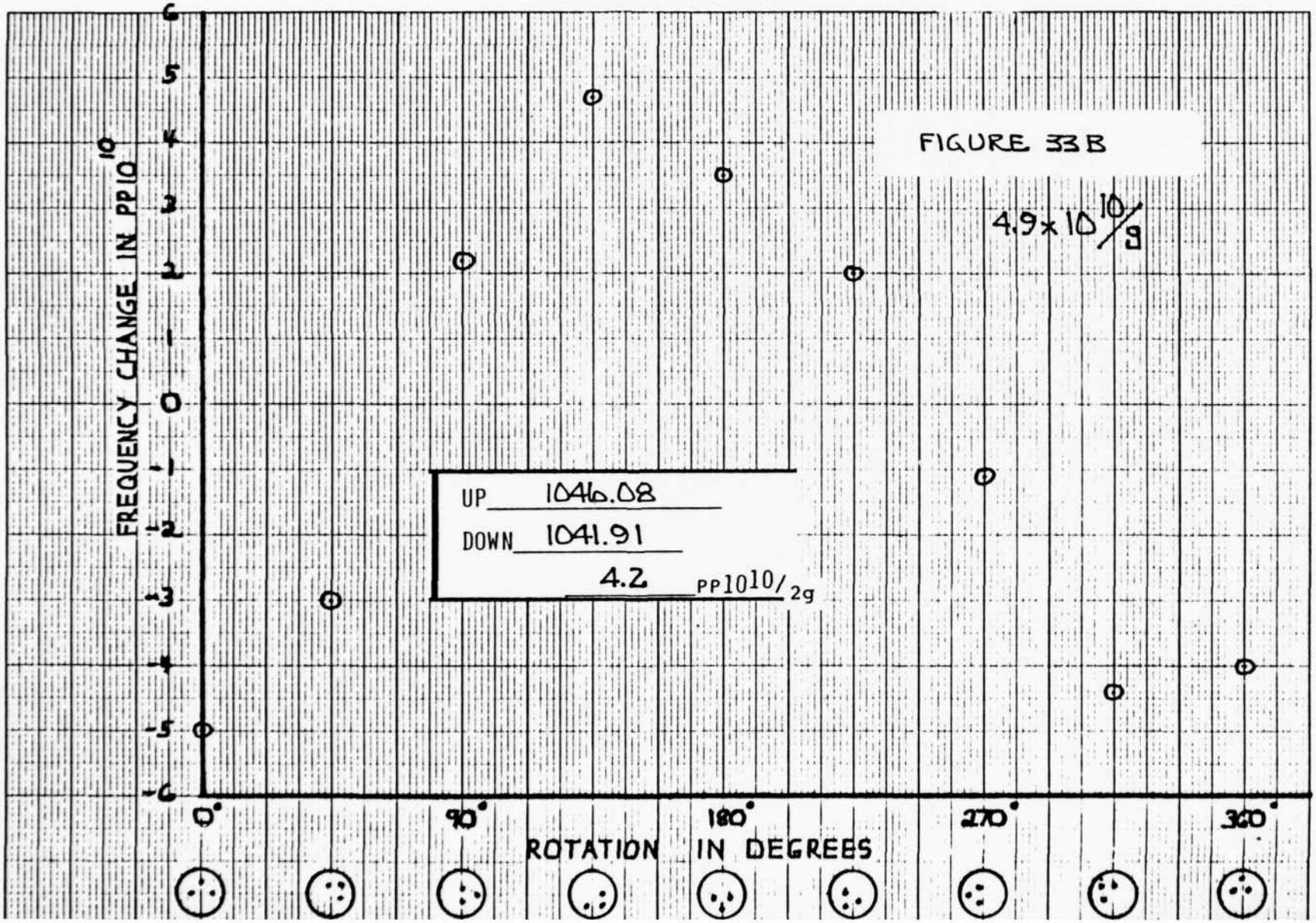

FIGURE 33B

SERNO. 4185 10.230400/3/SC DATE 9/5/80

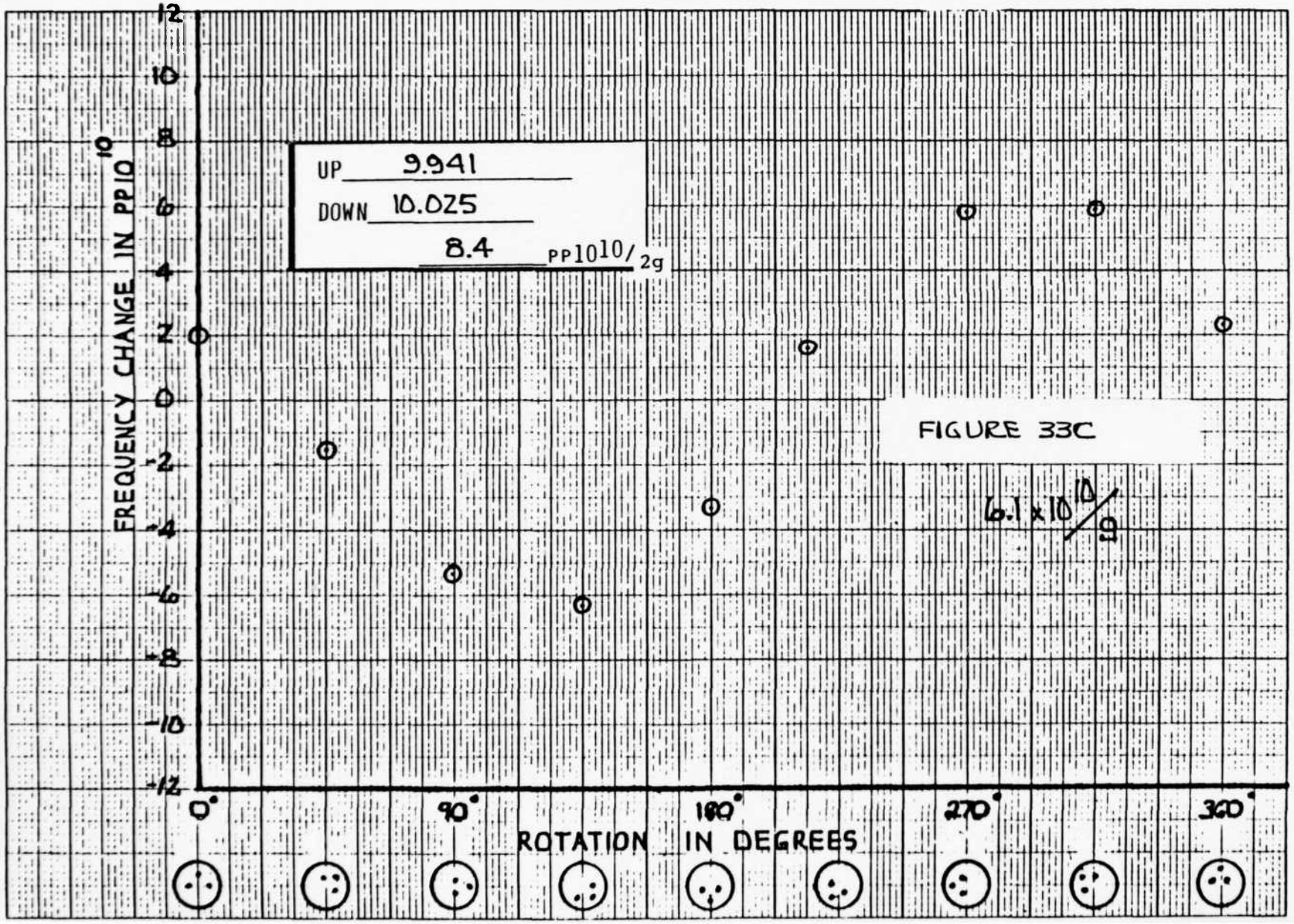

FIGURE 33C

SER NO. 4187 10.230400/3/SC DATE 9-5-80

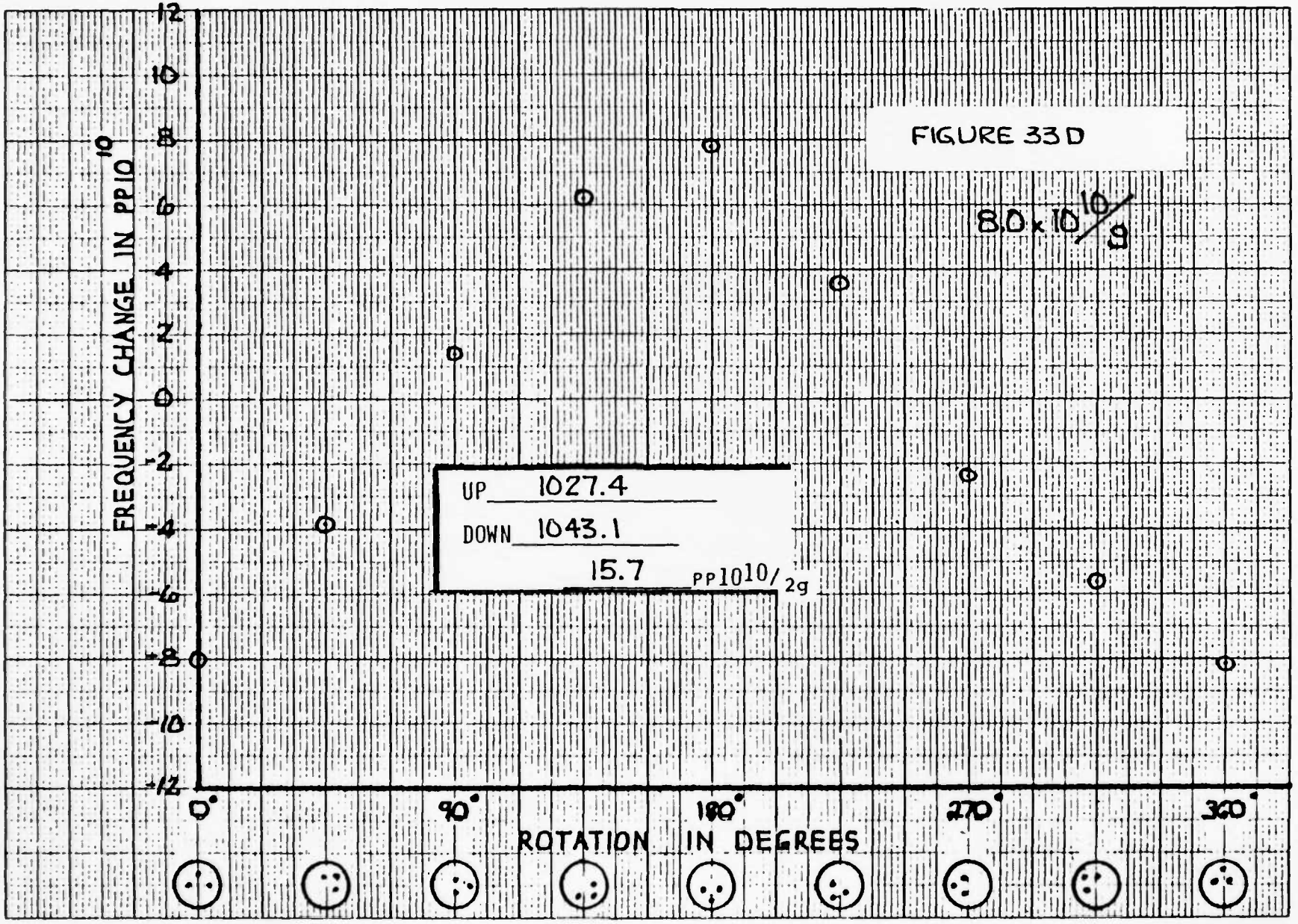

FIGURE 33 D

CRYSTAL	Γ_X	Γ_Y	Γ_Z	$\lvert\vec{\Gamma}\rvert$ IN PP10^{10}/g	TURNOVER TEMPERATURE	RESISTANCE (Ω)
P6116	+1.84	+ .5	-5.25	5.59	62°C	75
P6168	-2.5	-7.34	-4.17	8.80	77°C	85
P6170	-5.33	+3.83	-8.25	10.54	78°C	80
P6171	-2.5	+11.5	-11.5	16.45	92°C	80
P6332	-3.84	-3.25	-4.5	6.75	77°	80
P6334	-3.67	+5.34	+2.75	7.04	80°C	75
P6343	-3.33	+6.0	-3.5	7.7	68°C	105
P6345	+6.5	+1.17	+2.5	7.06	STK	80
BC6350	+3.0	-7.0	-.5	7.63	64°C	80
BC6351	+8.0	-1.17	13.25	15.52	70°C	110
2861	-2.34	-3.34	-.25	4.09	90°C	95
3242	+8.84	-4.17	-2.0	9.98	81°C	71
3886	-10.17	-4.34	+1.25	11.13	95°C	75
4182	-1.25	-.5	-4.75	4.94	62°C	70
4185	+4.34	-6.0	-5.0	8.94	59°C	70
4192	-2.5	+1.67	-2.75	4.07	63°C	95
4571	+1.67	-5.17	-13.5	14.55	75°C	90
4572	+1.0	+2.0	-18.0	18.14	50°C	77
9574	+.33	-5.5	-12.25	13.43	76°C	77
4743	+7.0	-5.0	-11.0	13.96	73°C	75
4744	+10.33	-1.5	-9.75	14.28	76°C	79
4746	+1.8	-6.5	-13.25	14.87	72°C	77
4747	-5.17	-2.34	-5.75	8.08	50°C	81
4748	-.5	+1.0	-4.75	4.88	>100°C	125
4750	+3.2	-7.9	-13.5	15.97	75°C	80
6179	+6.84	+1.84	-3.17	9.78	>100°C	85
6189	-3.84	-5.17	+3.5	7.33	78°C	80
6191	-3.67	-4.33	-10.5	7.00	90°C	80

FIGURE 34

MAGNITUDE OF THE ACCELERATION SENSITIVITY VECTOR FOR 10 MHz, 3RD OVERTONE CRYSTAL UNITS

CRYSTAL ASSEMBLY FINAL DATA SHEET

P/N _____ SPEC: _____ NOM. FREQ: 10.054 ; 10.23 MHz PROJ: 7554 FSO: VAR

S/N	f_s @ ____ °C	R_s Ω	f_p ____ pF; ____ °C	Δf (Hz)	C_o (pF)	C_1 x10^{-11} F	Q x10^{+6}	T.O. TEMP.	ACCELERATION PP10^{10}/g RADIAL	ACCELERATION PP10^{10}/g UP-DOWN	Δf P-P (PPM)
2861	10054044	135	10.054075	33	3.4	.233	1.26	85			
3142	10.054104	71	10.054128	24	3.6	1.71	1.30	81			
3886	10.054090	75	10.054110	20	3.85	1.426	1.48	95			
4182	10.230325	70	10.230345	20	3.7	1.43	1.55	62			
4192	10.230281	66	10.230306	25	3.1	1.76	1.3	63			
4571	10.057577	85	10.057584.6	7.6	2.6	.54	3.4	75			
4572	10.054188	77	10.054208	20	4.5	1.45	1.42	~50			
4574	10.054114	77	10.054134	20	4.5	1.45	1.42	76			
4743	10.054134	75	10.054154	20	4.5	1.45	1.46	73			
4744	10.054122	79	10.054142	20	4.5	1.45	1.38	76			
4746	10.054158	77	10.054178	20	4.5	1.45	1.42	72			
4747	10.054188	81	10.054208	20	4.5	1.45	1.35	~50			
4748	10.054144	125	10.054164	20	4.5	1.45	.87	72			
4750	10.054134	80	10.054154	20	4.5	1.45	1.36	75			
4185	10.230354	70	10.230375	21	3.7	1.51	1.47	59			

TESTED BY: R M. DATE: 9/13/81

A26910-FOR

FIGURE 35A

CRYSTAL ASSEMBLY FINAL DATA SHEET

P/N _____ SPEC: _____ NOM. FREQ: 10.054 MHz PROJ: 7554 PSO: VAR.

S/N	f_s @ 25 °C	R_s Ω	f_p 33 pF; 25 °C	Δf (Hz)	C_o (pF)	C_1 x10^{-4} F	Q x10^{+}	T.O. TEMP.	ACCELERATION PP10^{10}/g RADIAL	ACCELERATION PP10^{10}/g UP-DOWN	Δf P-P (PPM)
P6168	10.054083	85	10.054104	21	3.5	1.52	1.23	77°			
P6170	10.054083	80	10.054104	21	3.5	1.52	1.30	78°			
P6171	10.054057	80	10.054056	19	3.5	1.38	1.43	92°			
6179	10.054022	85	10.054041	19	2.8	1.35	1.38	110°			
6189	10.054136	90	10.054118	22	2.8	1.57	1.26	78°			
6191	10.054056	70	10.054076	20	2.8	1.42	1.38	90°			
P6332	10.054124	80	10.054148	24	3.5	1.69	1.17	70°			
P6334	10.054110	90	10.054130	20	3.5	1.41	1.40	77°			
P6343	10.054183	105	10.054205	22	3.5	1.60	.94	68°			
P6345	10.054215	80	10.054237	22	3.5	1.60	1.23	62°			
AC6350	10.054202	80	10.054224	22	3.5	1.60	1.23	64°			
AC6351	10.054166	110	10.054188	22	3.5	1.60	.90	70°			
P6116	10.054112	85	10.054133	21	2.65	1.49	1.25	62°			

TESTED BY: [illegible] DATE: 10/13/81

A26910-FOR

FIGURE 35B

CRYSTAL	FREQUENCY	Γ_X	Γ_Y	Γ_Z	$\lvert\vec{\Gamma}\rvert$	RESISTANCE	T.O.	MOUNT	DIOPTER	BOND METHOD
4749	10.054 MHz	Unstable Frequency after 24 hours in oscillator				77	77	Low Profile Diamond	1 3/4	Epoxy
4750	10.054 MHz	+ 3.2	-13.5	- 7.9	15.97	75	73	"	1 3/4	Epoxy
4751	10.054 MHz	+ 5.17	-14.75	-10.5	18.8	79	76	"	1 3/4	Epoxy
4936	10.054 MHz	Unstable after 24 hours in oscillator								
6610	10.054 MHz	- 6.0	- 2.0	+ 3.17	7.07	88	None	"	"	Epoxy
6611	10.054 MHz	- 4.5	- 7.5	- 1.75	8.9	83	None	"	"	Epoxy
6612	10.054 MHz	- 2.17	- 9.0	+ 5.67	10.9	90	None	"	"	Epoxy
6614	10.054 MHz	+ 1.5	+ 1.25	+ 9.8	10.0	77	None	"	"	Epoxy
6616	10.054 MHz	+ 9.25	- 5.5	+ 6.17	12.4	270	None	"	"	Epoxy
6617	10.054 MHz	- 2.0	+ 2.25	+ 2.8	4.1	72	>100	"	"	Epoxy
6626	10.054 MHz	- .67	- 2.25	- 2.7	3.6	77	None	"	"	Epoxy
6628	10.054 MHz	+12.0	- 3.0	- 4.0	13.0	73	None	"	"	Epoxy
6629	10.054 MHz	+10.5	+ 4.25	- 5.8	12.72	73	None	"	"	Epoxy
6631	10.054 MHz	- 3.2	+ 2.5	+ 6.2	7.41	74	None	"	"	Epoxy

11.51 Average

5.84 Standard Deviation

FIGURE 36

ACCELERATION SENSITIVITY VECTOR COMPONENTS AT 10 MHz

CRYSTAL	FREQUENCY	Γ_X	Γ_Y	Γ_Z	$\lvert\vec{\Gamma}\rvert$	RESISTANCE	T.O.	MOUNT	DIOPTER	BOND METHOD
6634	10.054 MHz	- 6.6	+ 1.25	- 1.6	6.90	81	None	"	"	Epoxy
6635	10.054 MHz	- 6.4	+ 7.5	+ 3.4	10.43	74	>100	"	"	Epoxy
6637	10.054 MHz	+ 5.3	- 4.0	- 1.8	7.45	72	None	"	"	Epoxy
6639	10.054 MHz	+10.0	- 1.75	+10.8	14.82	70	None	"	"	Epoxy
6666	10.054 MHz	- 2.1	- 1.75	+ 4.8	5.28	74	None	"	"	Epoxy
6669	10.054 MHz	- 6.5	+ 4.5	+11.4	13.87	83	None	"	"	Epoxy
6670	10.054 MHz	- 3.4	+ 2.25	+ .8	4.15	79	None	"	"	Epoxy
6950	10.054 MHz	- 2.2	+ 3.5	+ 3.4	5.35	71	>100	"	"	Epoxy
6952	10.054 MHz	- 3.2	+ 3.25	+ 4.7	6.54	100	99	"	"	Epoxy
6953	10.054 MHz	+ .6	+ 9.5	+ 4.7	10.62	108	92	"	"	Epoxy
6955	10.054 MHz	+18.1	+ 5.5	+ 1.4	19.0	153	95	"	"	Epoxy
6956	10.054 MHz	Missing	Leads			111	>100	"	"	Epoxy
6957	10.054 MHz	Missing	Leads			80	>100	"	"	Epoxy
6960	10.054 MHz	+ 8.8	+ 1.75	+11.7	14.7	73	>100	"	"	Epoxy
6962	10.054 MHz	-12.9	+11.25	-19.3	25.8	73	70	"	"	Epoxy
7456	10.054 MHz	+23.8	+ 7.0	+ .3	24.81	80	72	"	"	Epoxy

11.33 Average

5.89 Standard Deviation

FIGURE 36 - (CONTINUED)

ACCELERATION SENSITIVITY VECTOR COMPONENTS AT 10 MHz

100	19999.619	32	41	116	.69	82	20000	067	6.13
100	669	33		119	.67	75		020	–
102	585	36		130	.60	85		011	–
135	495	33		119	.50	7100		083	652
115	19999.090	33	29	115	.60	80	19999	489	5.66
145	317	33		115	.48	98		900	–
180	170	34		119	.37	76		545	–
190	670	34		119	.35	85	20000	100	–
135	508	32		116	.51	7100		163	8.48

APPENDIX I

"FURTHER DEVELOPMENTS ON SC CUT CRYSTALS"

B. GOLDFRANK
A. WARNER

FURTHER DEVELOPMENTS ON 'SC' CUT CRYSTALS

Bruce Goldfrank and Art Werner

Frequency Electronics, Inc.
New Hyde Park, New York 11040

Introduction

'SC' cut crystals have found their way into many new designs. The applications, though many and varied, center around the requirements of good 'g' sensitivity, resistance to radiation, fast warmup and good temperature characteristics. The temperature and strain effects on the 'SC' cut crystal are such that a large improvement over AT cut crystals is possible. In particular, data will be given on the improvement in radiation resistance of the 'SC' over the 'AT'.

In order to produce a successful SC crystal unit, i.e., one that exploits this design to the fullest, significant changes in design philosophy, design parameters, measuring techniques, testing methods, and production tools must be made. Three of the more important changes involve angle control prior to final lapping, angle measurements, and frequency adjustment. Where low 'g' sensitivity is important, the crystal plates must be thermo-compression bonded using small, uniform, very precisely located mounting spots.

Orientation

That the orientation of the plate must be closely controlled can be understood when we consider the typical AT frequency versus temperature curve. The center of the curve which is the inflection point, is at room temperature, and as the specified operating temperature goes higher, angle control becomes easier. For the SC, the inflection point is near 100°C and as the operating temperature approaches that point the angle control becomes difficult. 70°C to 80°C zero temperature coefficient (ZTC) for the SC cut is like 40°C to 50°C for the AT cut. At 80°C, one minute of arc error can shift the ZTC by 20°C. The benefit is, of course, that once angle control is achieved the temperature curve is much flatter.

Figure 1 shows a quartz bar and the steps of orientation, following the IEEE standard nomenclature, Y X w 1 tϕθψ. Visualize a starting plate which is a Y cut, rotate it about the Z axis by the angle ϕ and then rotate it about its new length, X', by the angle theta. The usual illustrations show the plate rectangular in shape. The final doubly oriented plate is usually shown the same size and shape as the starting plate. However, one can see that if we arrange to saw the

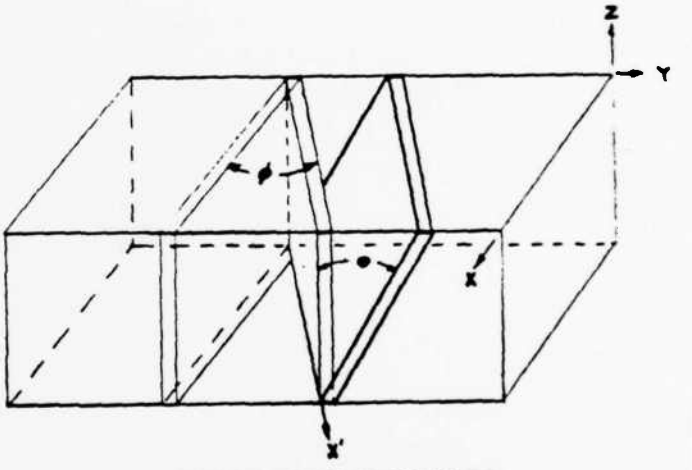

QUARTZ BAR SHOWING ROTATION AND TILT REQUIRED TO YIELD 'SC' BLANK

Figure 1. Stages of Orientation for a YXwlt ϕθψ Blank

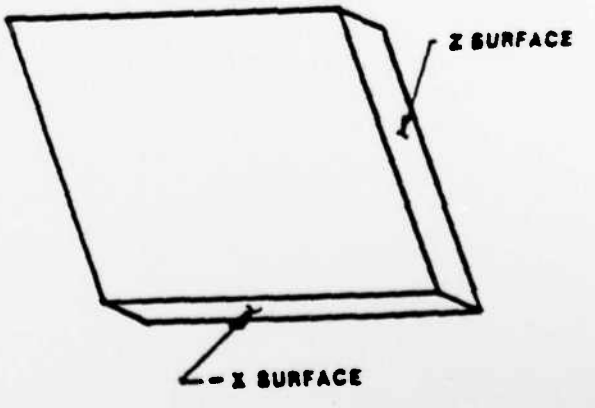

'SC' CUT CRYSTAL BLANK AS CUT FROM BAR

Figure 2. Quartz Blank As Cut From a Y Bar

Proc. 34th Ann. Freq. Control Symp., USAERADCOM, Ft. Monmouth, NJ 07703, May 1980.

doubly oriented plate from the bar, the shape will not be rectangular but will be as shown in Figure 2. If this were an AT, usual practice would be to simply mount it in the X-ray with the X axis vertical and compare the crystal face with the nearby 01.1 crystal plane at 38° 12.7'. However, with the SC we must first "undo" the ϕ angle, that is tilt the plate until the 01.1 plane is in a vertical position. The tilt itself is not particularly critical, but now the mounting flat, or if you will, the rotation of the plate about its thickness, becomes extremely critical, since this rotation will now tilt the reference plane.

Our answer to this problem is to highly correct the -X and one Z surface of the quartz bar itself before cutting. This is straight forward since, of course, there are X-ray planes parallel to these surfaces. These highly corrected surfaces are then used not only to orient the bar in the saw, but also to orient the blank in the X-ray goniometer.

Now, which edge surface should we use for the X-ray reference flat? The X' axis lies in the Z surface, some 14° away from using the -X surface as a reference flat and the X' would be the normal choice.

In either case, the equation to convert from the angle measured by the X-ray, to the specified θ angle is fairly simple, but it turns out there is an advantage to using the -X surface 14° away from the X' to locate the axis about which the X-ray angle is to be measured.

Figure 3 shows the relationship between the specified θ angle for various ϕ angles. The outer curve shows the equation developed by Ballato and Lefrate, and the other two curves show the corresponding angles θ' and θ'' measured by the tilt-back method for both X' axis and the -X surface. We can see that the angle measured using the -X surface, the upper curve, is much closer to the 38° 13' reference plane, even closer than that of the AT. Also we can see the slope is about 1 in 6 or 6' error in measuring ϕ results in 1' error in measuring θ. You may also have noticed that for the SC cut at ϕ = 23°, that the 14° shift in reference flat location corresponds to a 5 or 6 degree shift in indicated angle, or almost 2 to 1. Two minutes error in reference flat equals one minute error in angle measurement. To keep this error to an absolute minimum, we use, as indicated earlier, the actual corrected surface generated on the quartz bar before it is cut. In addition we use a special jig that avoids any error due to chipping at the edges. Figure 4 shows the tilt back vacuum jig used with the X-ray. The reference surface makes contact along a line away from the crystal edge. Figure 5 shows this reference contact a little more clearly. Repeatability using this method is about 10 seconds of arc. The ϕ angle is measured by a 90° turn of the quartz blank. No tilt is needed in this case, because the X-ray plane in this position is within 1-1/2 degrees of vertical, again closer than the AT for this measurement.

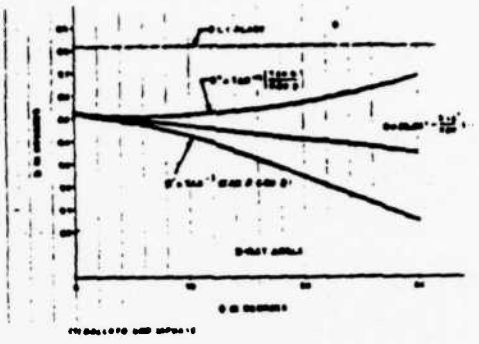

Figure 3. Relationship Between Specified : and : Angles and Those Measured By The Tilt-Back X-ray Method

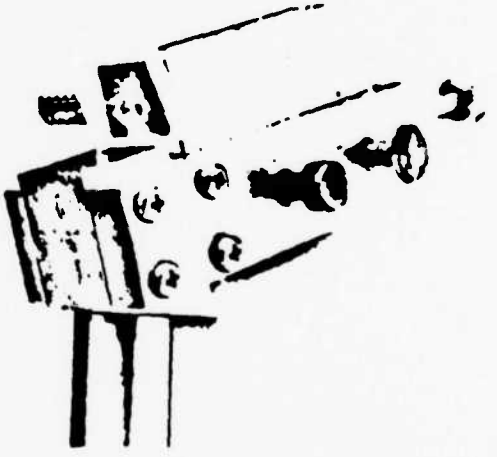

Figure 4. Tilt-Back Vacuum Jig Used With The Double-Crystal X-ray Goniometer

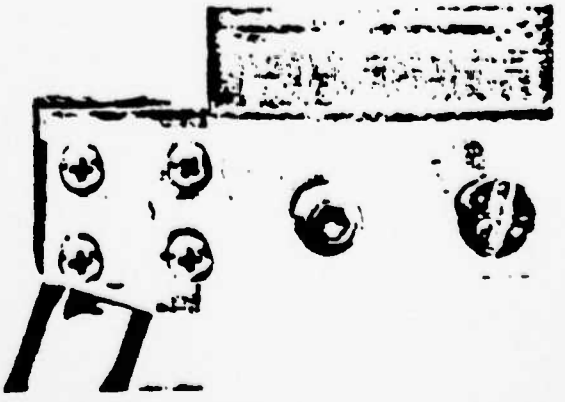

Figure 5. Tilt-Back Jig Showing -X Surface Contact

Figure 6 shows the precision saw. The setting is accomplished by a tilt and a rotation. Figure 7 is another view. One advantage of the tilt and rotation, rather than a double tilt is that the tilt and the rotation angles are exactly those measured by the X-ray. So necessary corrections to the saw table are directly applied from the X-ray reading. To obtain actual specified θ and ϕ angles, in practice, it is only necessary for the operator to enter the X-ray dial reading into a pre-programmed calculator and push the button.

Advantages of -X Surface Reference and Tilt Method of Orientation

1. An existing double crystal X-ray goniometer set for AT cut can be used with no change other than the tilt jig.
2. The angle is close enought to 01.1 plane for calibrating of standards by a turnover method.
3. Orientation of the sensitive reference flat is generated right on the quartz bar before cutting.
4. The ϕ angle is determined without a tilt jig and is simply measured by the X-ray.
5. By using a standard reference crystal, accuracies of a few seconds of arc are possible.
6. There is a direct correspondence between saw table angles and the angles measured by the X-ray.
7. Specified angles are obtained easily by using a simple programmed calculator.
8. The 14° psi angle generated automatically turns out to be the correct mounting point for the crystal plate.

Frequency Adjustment

The fact that the inflection point of the SC temperature frequency curve is above the operating temperature makes room temperature frequency adjustment a disaster. The slope is about 10 Hz per degree at 5 MHz. In addition frequency adjustment by circuit means is limited to about 1/4 of that of the AT. Therefore frequency adjustment at or near the temperature at which the crystal is to be operated is imperative. Figure 8 shows a small heater used in the vacuum deposition chamber. Temperature sensing control is by a thermistor bridge, the lead wires from the crystal are of special material and pass thru the temperature controlled block on their way to a network which sets the operating phase conditions. Deposition is by evaporation from a small tungsten filament.

Crystal Mounting

Figure 9 shows an experimental approach to thermo-compression (TC) ribbon mounting of the crystal plate. The ribbon is nickel, and it has a gold triangular strip bonded thereon. The TC bond will be gold to gold, and in the shape of a long thin rectangle, about 5 x 30 mils. This method permits a better location of the mounting points with respect to the center of the plate, and also permits TC bonding to very thin plates.

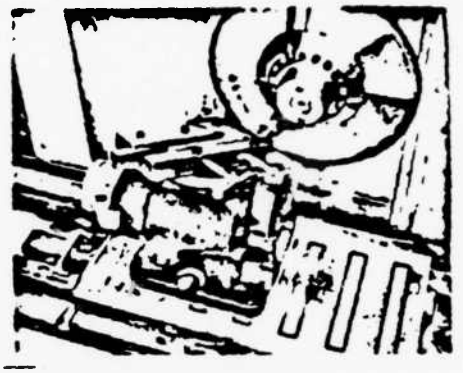

Figure 6. One View of the Precision Saw

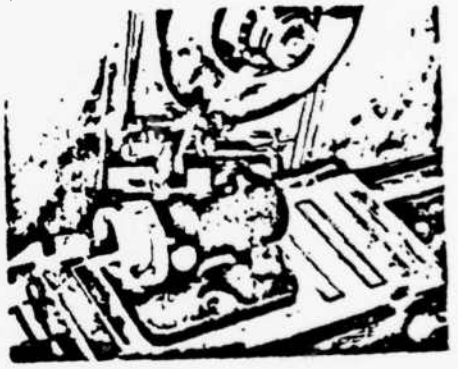

Figure 7. One View of the Precision Saw

Figure 8. Crystal Unit Heater For Cold Evaporation in Vacuum

Figure 10 is a photo of one such bond on e 5 MHz 5th overtone plete. Figure 11 is a drawing of a typicel thermocompression bond. Recent discussions with end calaculetions by Prof. Peter Lee, of Princeton University, have indicated the extreme importance of the mounting points in obtaining a low 'g' eensitivity crystal unit. He indicetes a ψ angle near -15° es optimum for a 3 point 90° mount. It ie interesting to note that the naturel angle generated in cutting the blank, (-14.8°) which Frequency Electronics uses, the experimental angle reported by Kusters, Adems, and others of Hewlett Packard in 1977, end Peter Lee's calculated angle ere ell essentielly the aame. I believe the naturally generated angle is the correct one, but further experimentation will be necessary with precisely mounted units, to verify this.

Radistion Effects

An unexpected bonus came to light when some 24 MHz SC units in oscillators intended for use in the Galileo Probe of Jupiter were subjected to radiation of 1.0 megareds. The SC units changed 1 part in 10^{14}/rad versus 2 parts in 10^{12} per rad for AT units. This is about 2 orders of magnitude improvement in rediation susceptibility. This agsin needs further study.

Conclusion

Figure 12 shows e greph of one 5 MHz doubly contoured SC unit made et Frequency Electronics, Inc. eubjected to e 2G ecceleration by e simple turn-over test. Plate up to plete down was $1PP10^{11}$. Rotation in the vertical plane shows less than $1PP10^{10}$ per G. Future etudies will be eimed et increesing the yield of euch units.

Acknowledgment

This work was supported in part by a grant from USAERDCOM, #DAAK20-79-C-0272.

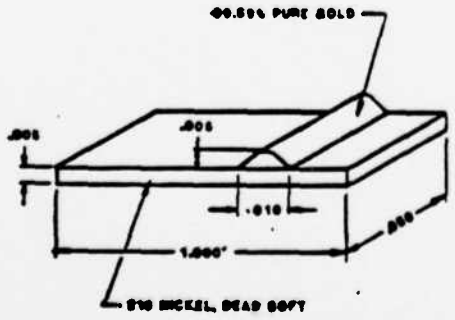

Figure 9. Experimentsl Gold Bonded Nickel Mounting Ribbon

Figure 10. Experimental Thermo-Compression Bond To A 5 MHz SC Plate

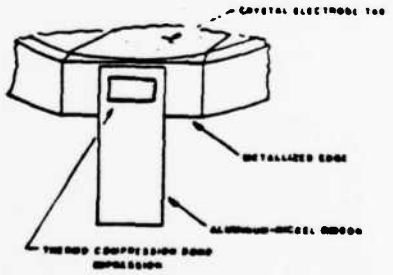

Figure 11. Typicel Thermo-Compression Bond

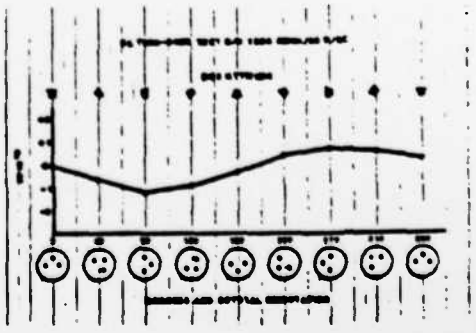

Figure 12. Turn-Over Test of One 5 MHz, 5th Overtone SC Unit Showing a 'g' Sensitivity of Less Than $1PP10^{10}$

18 January 1982

FREQUENCY CONTROL BRANCH DISTRIBUTION LIST

Dr. Bernard Sklar
Aerospace Corporation
MS 120-2210
Box 92957
Los Angeles, CA 90009

Dr. Charles Volk
Aerospace Corporation
Box 92957
Los Angeles, CA 90009

Mr. Andrew Przedpelski
ARF Products
2559 75th Street
Boulder, CO 80301

Mr. Hal Thicksten
ASU R&D Corporation
512 North Main Street
Orange, CA 92668

Mr. Robert Ellis
AUSTRON, Inc.
1915 Kramer Lane
Austin, TX 78758

Mr. E. J. Alexander
Bell Laboratories
555 Union Boulevard
Allentown, PA 18103

Mr. E.D. Kolb
Bell Laboratories
600 Mountain Avenue
Murray Hill, NJ 07974

Mr. T. R. Meeker
Bell Laboratories
555 Union Boulevard
Allentown, PA 18103

Mr. Harold Jackson
Bendix Communications Division
East Joppa Road
Baltimore, MD 21204

Philip E. Talley
Aerospace Corporation
Box 92957
Los Angeles, CA 90009

Mr. S. Kaat
Bliley Electric Company
2545 W. Grandview Blvd.
Erie, PA 16508

Mr. Kirk Dance
CINOX
4914 Gray Road
Cincinnati, OH 45232

Mr. Canon Bradley
Colorado Crystal Company
2303 W. 8th Street
Loveland, CO 80537

Dr. W. D. Beaver
Comtec Laboratory
16871 Noyes Avenue
Irvine, CA 92714

Mr. George Bistline
620 Belvedere Street
Carlisle, PA 17013

Dr. Virgil E. Bottom
3441 High Meadows
Abilene, TX 79605

Mr. Charles Stone
Brightline Corp.
P.O. Box 1016
Cedar Park, TX 78613

Jerry P. Middendorf
Cincinnati Electronics
2630 Glendale-Milford Road
Cincinnati, Ohio 45241

Mr. Larry Berberich
Cirtech Corporation
P.O. Box 96
15237 Cherry Street
Stanley, Kansas 66223

Mr. Kelly Scott
Crystal Systems, Inc.
P.O. Box 225
Chardon, OH 44022

Mr. Curt Bowen
CTS Knights, Inc.
400 Reimann Avenue
Sandwich, Illinois 60548

Mr. J.F. Silver
CTS Knights, Inc.
400 Reiman Avenue
Sandwich IL 60548

Mr. Hugo Fruehauf
Efratom California, Inc
18851 Bardeen Avenue
Irvine, CA 92715

George D. Verdelin
Eaton Corporation
Elec. Inst. Div. - R&D Center
612 North Mary Avenue
Sunnyvale, CA 94086

Mr. E.B. Lewis
EBL Co., Inc.
91 Tolland Street
East Hartford, CT 06108

Mr. William Riley
EG&G-Rubidium Clocks
35 Congress Street
Salem, MA 01970

Mr. Maurice White
Electrodynamics, Inc.
5625 Fox Ridge Drive
Mission, KS 66201

Mr. J. J. Colbert
Electronic Crystals Company
1153 Southwest Blvd.
Kansas City, KS 66103

Mr. Donald Peters
Erie Technological Products
453 Lincoln Street
Carlisle, PA 17013

Mr. Carl Leonard
Frequency Control Products Inc.
61-20 Woodside Avenue
Woodside, NY 11377

Mr. Charles Stone
Brightline Corp
P.O. Box 1016
Cedar Park, TX 78613

Dr. D. Emmons
Frequency & Time Systems, Inc.
23 Tozer Road
Beverly, MA 01915

Dr. Helmut Hellwig
Frequency & Time Systems, Inc.
23 Tozer Road
Beverly, MA 01915

Mr. Martin Bloch
Frequency Electronics, Inc.
55 Charles Lindberg Blvd.
Mitchel Field, NY 11553

Mr. A. W. Warner
Frequency Electronics, Inc.
55 Charles Lindberg Blvd.
Mitchel Field, NY 11553

Mr. Butch Tysinger
Crystek Corp
P.O. Box 06135
Ft. Myers, FL 33906

Mr. Jack Keres
General Electric Company
P.O. Box 11508
St. Petersburg, FL 33733

Mr. Thomas Snowden
General Electric Company
P.O. Box 11508
St. Petersburg, FL 33733

Mr. Robert Ney
General Electric Company
P.O. Box 11508
St. Petersburg, FL 33733

Mr. Thomas Wagner
General Electric Company
P.O. Box 11508
St. Petersburg, FL 33733

Technical Data Library
General Electric Company
P.O. Box 11508
St. Petersburg, FL 33733

Mr. Raymond H. Green
Greenray Industries
840 West Church Road
Mechanicsburg, PA 17055

Dr. Tae M. Kwon
Litton Guidance & Control Systems
Research & Advanced
Development Engineering
5500 Canega Avenue
Woodland Hills, CA 91365

Mr. David L. Hessick
Magnavox Gov't & Ind'l Elec Co.
Advanced Products Division
2829 Maricopa Street
Torrance, CA 90503

Mr. Ed Boise
McCoy Electronics
Chestnut & Watts Streets
Mt. Holly Springs, PA 17013

Mr. Walter D. Galla
McCoy Electronics
Chestnut & Watts Streets
Mr. Holly Springs, PA 17013

Mr. C.E. Hagen
Microsonics, Inc.
60 Winter Street
Weymouth, MA 02188

Mr. J. K. Miller
J.K. Miller Company
80 Wabash Street
Pittsburg, PA 15220

Mr. Gene O'Sullivan
Mitre Corporation
MS E035
P.O. Box 208
Bedford, MA 01730

Dr. Myron Weinstein
Mictron, Inc.
P.O. Box 10126
Sarasota, FL 33578

Mr. O.R. Montgomery
Monitor Products Company, Inc.
P.O. Box 1966
Oceanside, CA 92054

Dr. J.F. Balascio
Motorola, Inc.
P.O. Box 279
Carlisle, PA 17013

Mr. Larry Conlee
Motorola, Inc.
2553 N. Edgington Avenue
Franklin Park, IL 60131

Mr. L.N. Dworsky
Motorola Inc.
8000 W. Sunrise Blvd
Plantation, FL 33322

Mr. D. Reifel
Motorola, Inc.
2553 N. Edgington Avenue
Franklin Park, IL 60131

Mr. Roger Ward
Motorola, Inc.
8000 W. Sunrise Blvd.
Ft. Lauderdale, FL 33322

Mr. Del Gaines
M-TRON Industries, Inc.
East Highway 50
Yankton, OS 57078

Mr. J. Holmbeck
Northern Engineering Labs
357 Beloit Street
Burlington, WI 53105

Prof. O.E. Newell
Northern Illinois University
DeKalb, IL 60115

Dr. L.E. Halliburton
Oklahoma State University
Department of Physics
Stillwater, OK 74074

Mr. N. Broadbent
Ovenaire-Audio-Carpenter
706 Forrest Street
Charlottesville, VA 22901

Mr. Benjamin Parzen
3634 Seventh Avenue
San Diego, CA 92103

Prof. R.E. Newnham
Pennsylvania State University
252 Materials Research Lab
University Park, PA 16802

Mr. C. Jensik
Piezo Crystal Company
100 K Street
Carlisle, PA 17013

Dr. W.H. Horton
Piezo Technology, Inc.
2525 Shader Road
Orlando, FL 32804

Prof. P.C.Y. Lee
Princeton University
Dept. of Civil Engineering
Princeton, NJ 08540

Mr. H. Phillips
Q-Tech Corporation
2201 Carmelina Avenue
Los Angeles, CA 90024

Daryl Kemper
QUARTZTEK, Inc.
20 South 48th Avenue
Suite 2
Phoenix, AZ 85043

Mr. T.E. Parker
Raytheon Research
28 Seyon Street
Waltham, MA 02154

R. Michel Zilberstein
Raytheon Company
Microelectronics Dept.
465 Centre Street
Quincy, MA 02169

Mr. F. Brandt
Reeves Hoffman Division
400 W. North Street
Carlisle, PA

Mr. D.V. Kingery
Reeves-Hoffman
400 W. North Street
Carlisle, PA 17013

Prof. H.F. Tiersten
Rensselaer Polytechnic Inst.
Jonsson Engineering Center
Troy, NY 12180

Mr. E.J. Staples
Rockwell Science Center
1049 Camino Dos Rio
Thousand Oaks, CA 91360

Mr. Marvin Frerking
Rockwell International
Collins Tele. Prod. Div.
855 35th Street, N.E.
Cedar Rapids, IA 52406

Mr. J.M. Ronan
J.M. Ronan Assoc., Inc.
44 Cindy Lane
Wayside, NJ 07712

Mr. T.J. Young
Sandia Laboratories
P.O. Box 5800
Albuquerque, NM 87185

Mr. Jack Saunders
Saunders & Assoc.
7440 E. Karen Drive
Scottsdale, AZ 85251

Mr. O.E. Lussier
Savoy Electronics Company
P.O. Box 5727
1175 NE 24th Street
Ft. Lauderdale, FL 33334

Dr. D. Kinloch
Sawyer Research
35400 Lakeland Blvd.
Eastlake, OH 44094

Dr. B. Sawyer
Baldwin Sawyer Crystals, Inc.
P.O. Box 96
Gates Mills, OH 44040

Mr. J. H. Sherman
2022 Woodcrest Drive
Lynchburg, VA 24503

Mr. Herbert Rogall
Singer
90 New Dutch Lane
Fairfield, NJ 07006

Dr. E. Hafner
881 Sycamore Avenue
Tinton Fall, NJ 07724

Mr. Joseph H. Geiger
Hazeltine Corp.
Greenlawn, NY 11740

Dr. Donald Hammond
Hewlett-Packard Company
1501 Page Mill Road
Palo Alto, CA 94304

Mr. C.A. Adams
Hewlett-Packard Company
5301 Stevens Creek Blvd.
Santa Clara, CA 95050

Mr. Mike Fisher
Hewlett-Packard Co.
5301 Stevens Creek Blvd.
Santa Clara, CA 95050

Mr. J.A. Kusters
Hewlett-Packard Company
5301 Stevens Creek Blvd.
Santa Clara, CA 95050

Mr. Robert Birrell
P.R. Hoffman Company
321 Cherry Street
Carlisle, PA 17013

Dr. T.R. Joseph
Hughes Aircraft Company
Bldg. 600/F259
P.O. Box 3310
Fullerton, CA 92634

Mr. H. E. Dillon
Hughes Aircraft Company
500 Superior Avenue
Newport Beach, CA 92663

Lloyd C. Tignor
Isotemp Research, Inc.
P.O. Box 3389
Charlottesville, Virginai 22901

Mr. J. Erasmus
JAN Crystals Co.
2400 Crystal Drive
Ft. Myers, FL 33907

Dr. Terry M. Flannagan
JAYCOR
11011 Torreyana Road
P.O. Box 85154
San Diego, CA 92138

Dr. Richard L. Sydnor
Jet Propulsion Laboratory
MS238-420
4800 Oak Grove Drive
Pasadena, CA 91109

Mr. J. Norton
Johns Hopkins University
Applied Physics Laboratory
Johns Hopkins Road
Laurel, MD 21810

Mr. Lauren J. Rueger
Johns Hopkins University
Applied Physics Laboratory, 4-326
Johns Hopkins Road
Laurel, MD 20810

Mr. Rolf Weglein
Hughes Aircraft Missile Systems Group
8433 Fallbrook Avenue
Canoga Park, CA 91304

Mr. Robert Kern
KERNCO, Inc.
28 Harbor Street
Danvers, MA 01923

Mr. Richard Bush
MIT Lincoln Laboratory
P.O. Box 73
Lexington, MA 02173

Mr. Lewis D. Collins
MIT Lincoln Laboratory
P.O. Box 73
Lexington, MA 02173

Mr. Paul McHugh
MIT Lincoln Laboratory
P.O. Box 73
Lexington, MA 02173

Mr. William C. Lindsey
Lincom Corporation
1543 Olympic Blvd
4th Floor
Los Angeles, CA

AD-A132 274 VIBRATION RESISTANT QUARTZ CRYSTAL RESONATORS(U) 1/2
FREQUENCY ELECTRONICS INC MITCHEL FIELD NY
B GOLDFRANK ET AL. NOV 82 DELET-TR-79-0272-F
UNCLASSIFIED DAAK20-79-C-0272 F/G 9/1 NL

END
DATE FILMED
*9 -83
DTIC

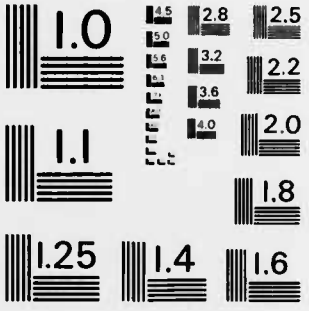

MICROCOPY RESOLUTION TEST CHART
NATIONAL BUREAU OF STANDARDS-1963-A

Mr. T. Sokol
Sokol Crystal Products, Inc.
121 Water Street
Mineral Point, WI 53565

Mr. Jurgen H. Staudte
391 S. Henning Way
Anaheim, CA 92807

Mr. W.J. Tanski
Sperry Research
100 North Road
Sudbury, MA 01776

John Fisher
Standard Crystal Corp
9940 Baldwin Place
El Monte, CA 91731

Dr. Shih S. Chuang
STATEK, Inc.
512 North Main Street
Orange, CA 92668

Mr. L.T. Claiborne
Texas Instrument Co.
P.O. Box 225936
Dallas, TX 75265

Mr. William F. Donnell
Tracor, Inc.
MS 6-1
6500 Tracor Lane
Austin, TX 78721

Mr. F. Sauerland
Transat Corporation
3713 Lee Road
Shaker Heights, OH 44120

Dr. Reynold Kagiwada
TRW DSSG
R1, 1086
One Space Park
Redondo Beach, CA 90278

Mr. M. Gilden
United Technology Res. Ctr.
Silver Lane
E Hartford, CT 06108

Mr. Neil Bernstein
Valpey-Fisher Company
75 South Street
Hopkinton, MA 01748

Mr. N. Benoit
VALTEC
75 South Street
Hopington, MA 01748

Mr. Stanley Tulgan
Vectron Laboratory Inc.
166 Glover Avenue
Norwalk, CT 06850

Mr. E.E. Simpson
Western Electric
1600 Osgood Street
N. Andover, MA 01845

Mr. Ivan Oak
Western Electric
1600 Osgood Street
N. Andover, MA 01845

Mr. D.J. Healey III
Westinghouse Inc.
P.O. Box 746, MS 294
Baltimore, MD 21203

Mr. David Larson
Sawyer Crystal Systems Inc.
1601 Airport Road
P.O. Box 2707
Conroe, TX 77301

Mr. B.R. McAvoy
Westinghouse R&D
1310 Beulah Road
Pittsburg, PA 15235

LT Karl Kovach YEE
AF Space Division
P.O. Box 92960
Worldway Postal Center
Los Angeles, CA 90005

CPT Demo Galanos
USAF Space Division, YEZ
P.O. Box 9260
Worldway Postal Center
Los Angeles, CA 90009

Mr. A.F. Armington
USAF
RADC/ESM
Hanscom AFB
Bedford, MA 01731

Dr. P.H. Carr
USAF
RADC/EEN
Hanscom AFB
Bedford, MA 01731

Mr. A. Kahan
USAF
RADC/ES
Hanscom AFB
Bedford, MA 01731

Dr. N. Yannoni
USAF
RADC/ESE
Hanscom AFB
Bedford, MA 01731

Mr. J. Plaisted
ASD/XRQ-NIS
Wright Patterson AFB, OH 45433

Dr. A. Ballato
USAERADCOM
ATTN: DELET-MA-A
Fort Monmouth, NJ 07703

Mr. R. J. Brandmayr
USAERADCOM
ATTN: DELET-MQ-R
Fort Monmouth, NJ 07703

Dr. R.L. Filler
USAERADCOM
ATTN: DELET-MQ-R
Fort Monmouth, NJ 07703

Mr. V.G. Gelnovatch
USAERADCOM
ATTN: DELET-M
Fort Monmouth, NJ 07703

Mr. J.G. Gualtieri
USAERADCOM
ATTN: DELET-MQ-R
Fort Monmouth, NJ 07703

Mr. J. Kosinski
USAERADCOM
ATTN: DELET-MQ-R
Fort Monmouth, NJ 07703

Mr. T. Lukaszek
USAERADCOM
ATTN: DELET-MA-A
Fort Monmouth, NJ 07703

Mr. G. Malinowski
USAERADCOM
ATTN: DELET-MQ-O
Fort Monmouth, NJ 07703

Mr. V. Rosati
USAERADOM
ATTN: DELET-MQ-O
Fort Monmouth, NJ 07703

Mr. S. Schodowski
USAERADCOM
ATTN: DELET-MQ-O
Fort Monmouth, NJ 07703

Dr. J.R. Vig
USAERADCOM
ATTN: DELET-MQ
Fort Monmouth, NJ 07703

Mr. W. Washington
USAERADCOM
ATTN: DELET-MQ-R
Fort Monmouth, NJ 07703

USDOE
Technical Information Center
P.O. Box 62
Oak Ridge, TN 37830

Mr. Andrew Chi
Code 810
NASA/GSFC
Greenbelt, MD 20771

Mr. F.L. Walls
National Bureau of Standards
325 Broadway
Boulder, CO 80303

Mr. David Philips
Naval Research Laboratory
Code 7524
4555 Overlook Avenue SW
Washington, DC 20375

Dr. Gernot Winkler
US Naval Observatory
34th & Massachusetts Ave, NW
Washington, DC 20390

Mr. Ralph Allen
Naval Electronic Sys Command
Code 51023
Washington, DC 20360

Dr. Allan Tarbell
PM SOTAS
DRCPM-STA-TM
Fort Monmouth, NJ 07703

Mr. Cary Fishman
PM SINCGARS
DRCPM-GARS-TM
Fort Monmouth, NJ 07703


DAT
FILM